Stable isotopes in leaf water of terrestrial plants

Lucas A. Cernusak[1], Margaret M. Barbour[2], Stefan K. Arndt[3], Alexander W. Cheesman[1], Nathan B. English[4], Taylor S. Feild[4], Brent R. Helliker[5], Meisha M. Holloway-Phillips[6], Joseph A.M. Holtum[4], Ansgar Kahmen[7], Francesca A. McInerney[8], Niels C. Munksgaard[9,10], Kevin A. Simonin[11], Xin Song[2], Hilary Stuart-Williams[6], Jason B. West[12], Graham D. Farquhar[6]

[1]College of Marine and Environmental Sciences
James Cook University, Cairns, Australia

[2]Centre for Carbon, Water and Food, Faculty of Agriculture and Environment
The University of Sydney, Camden, Australia

[3]School of Ecosystem and Forest Science
The University of Melbourne, Melbourne, Australia

[4]College of Marine and Environmental Sciences
James Cook University, Townsville, Australia

[5]Department of Biology
University of Pennsylvania, Philadelphia, USA

[6]Research School of Biology
The Australian National University, Canberra, Australia

[7]Department of Environmental Sciences- Botany
University of Basel, Basel, Switzerland

[8]Department of Earth Sciences
The University of Adelaide, Adelaide, Australia

[9]College of Science, Technology and Engineering
James Cook University, Cairns, Australia

[10]Research Institute for the Environment and Livelihoods
Charles Darwin University, Darwin, Australia

[11]Department of Biology
San Francisco State University, San Francisco, USA

[12]Department of Ecosystem Science and Management
Texas A&M University, College Station, USA

This article has been accepted for publication in *Plant, Cell & Environment* and undergone full peer review but has not been through the copyediting, typesetting, pagination and proofreading process which may lead to differences between this version and the Version of Record. Please cite this article as doi: 10.1111/pce.12703

ABSTRACT

Leaf water contains naturally occurring stable isotopes of oxygen and hydrogen in abundances that vary spatially and temporally. When sufficiently understood, these can be harnessed for a wide range of applications. Here, we review the current state of knowledge of stable isotope enrichment of leaf water, and its relevance for isotopic signals incorporated into plant organic matter and atmospheric gases. Models describing evaporative enrichment of leaf water have become increasingly complex over time, reflecting enhanced spatial and temporal resolution. We recommend that practitioners choose a model with a level of complexity suited to their application, and provide guidance. At the same time, there exists some lingering uncertainty about the biophysical processes relevant to patterns of isotopic enrichment in leaf water. An important goal for future research is to link observed variations in isotopic composition to specific anatomical and physiological features of leaves that reflect differences in hydraulic design. New measurement techniques are developing rapidly, enabling determinations of both transpired and leaf water $\delta^{18}O$ and $\delta^{2}H$ to be made more easily and at higher temporal resolution than previously possible. We expect these technological advances to spur new developments in our understanding of patterns of stable isotope fractionation in leaf water.

INTRODUCTION

In this review, we focus on how stable isotope ratios of oxygen and hydrogen vary in leaf water. The stable isotope composition of leaf water significantly influences isotopic signatures of a number of important biological and atmospheric processes. For example, the oxygen isotope composition of leaf water partly controls the oxygen isotope compositions of atmospheric CO_2 (Farquhar *et al.* 1993; Cuntz *et al.* 2003; Welp *et al.* 2011) and atmospheric O_2 (Dole *et al.* 1954; Hoffmann *et al.* 2004; Luz & Barkan 2011). Sugars and other metabolites formed in leaves incorporate the leaf water isotopic signal, which is then retained in structural organic compounds, such as cellulose (Saurer, Aellen & Siegwolf 1997; Roden, Lin & Ehleringer 2000; Barbour 2007; Gessler *et al.* 2014). The leaf water signal is also preserved in leaf waxes (Smith & Freeman 2006; Sachse *et al.* 2010; Kahmen *et al.* 2013a; Kahmen, Schefuss & Sachse 2013b), components of which can persist in the environment for millions of years (Eglinton & Eglinton 2008). Thus, leaf water derived isotopic signals can be useful for constraining models of the global carbon cycle, reconstructing past climates, retrospectively analysing plant physiological responses to the environment, and for assigning geographic origins to plant materials and plant-derived products (Dawson *et al.* 2002; West *et al.* 2006b). All of these various applications rely on a firm understanding of the mechanisms that control leaf water isotopic enrichment.

For plant water, isotopic abundances are generally expressed relative to the international standard VSMOW (Vienna Standard Mean Ocean Water) (Coplen 2011). This is accomplished using δ notation:

$$\delta_p = \frac{R_p - R_{Std}}{R_{Std}}, \quad (1)$$

where R_p is the isotope ratio (*e.g.*, $^{18}O/^{16}O$ or $^{2}H/^{1}H$) of a plant water sample and R_{Std} is that of the standard. The resulting δ values are typically multiplied by 1000, so that the relative deviation of the isotope ratio of the sample from that of the standard is expressed as per mil (‰).

The stable isotope composition of plant water is influenced firstly by the plant's source water; this is mainly water taken up by roots from the soil. Soil water for terrestrial plants generally derives from local precipitation. The stable isotope composition of precipitation can vary both geographically and temporally. The $\delta^{18}O$ and $\delta^{2}H$ of precipitation have been shown to vary in conjunction with temperature, altitude, latitude, distance from the coast, and with the amount of precipitation falling in a given event (Rozanski, Araguas-Araguas & Gonfiantini 1993; Araguas-Araguas, Froehlich & Rozanski 2000; Bowen 2010;

Munksgaard *et al.* 2012). A representation of geographic variation in the $\delta^{18}O$ and $\delta^{2}H$ of mean annual precipitation across the global land surface is shown in Figures 1A and 1B.

Any given precipitation event will mix into an existing soil water pool. Thus, although there can exist relatively large variation in $\delta^{18}O$ and $\delta^{2}H$ from one precipitation event to the next (Munksgaard *et al.* 2012; Munksgaard *et al.* 2015), the soil water pool being accessed by plants will likely be buffered to some extent against these short term variations. The extent to which the isotopic composition of the soil water pool can be linked to individual precipitation events is an area of current interest (Tang & Feng 2001; Brooks *et al.* 2010; Thomas *et al.* 2013; Gessler *et al.* 2014). It is particularly relevant, for example, to the detection of long-term records of tropical cyclone activity in tree rings (Miller *et al.* 2006), because tropical cyclones are predominantly associated with isotopically light precipitation (Gedzelman & Arnold 1994; Lawrence & Gedzelman 1996; Munksgaard *et al.* 2015). The isotopic composition of soil water can also be affected by evaporation. This causes the soil water near the evaporating front to become enriched in ^{18}O and ^{2}H compared to the soil water at depth (Allison, Barnes & Hughes 1983; Barnes & Allison 1983).

For the most part, the isotopic composition of water in non-transpiring plant organs (*i.e.*, roots, stems, etc.) has been shown to match that of the water available to the plant in the soil, indicating that there is little to no stable isotope fractionation associated with absorption of water by roots and transport in xylem (White 1989; Ehleringer & Dawson 1992; Dawson 1993). The exception to this rule is that $\delta^{2}H$ has been observed to shift with water uptake and/or transport in salt tolerant coastal plants (Lin & Sternberg 1993) and phreatophytic desert shrubs (Ellsworth & Williams 2007). No simultaneous $\delta^{18}O$ fractionation was observed, indicating that the cause of the isotope effect was specific only to hydrogen isotopes in water and not oxygen isotopes, or that the isotope effect for oxygen was too small to be detected.

Transpiration results in isotopic enrichment at the sites of evaporation within leaves. The isotopically enriched water can then diffuse away from the evaporative sites into other parts of the leaf. The resulting bulk leaf water enrichment generally shows a diurnal pattern, with a daily maximum in the early afternoon associated with the minimum daily relative humidity, and a daily minimum in the early morning reflecting a progressive relaxation of the enrichment through the night (Figure 2). Enriched leaf water can also be transported in the phloem to developing sink organs such as seeds (Figure 2). In the following sections, we

examine in detail the environmental and physiological controls over the stable isotope enrichment of the evaporative sites and the bulk leaf water.

LEAF WATER

Evaporative sites

Isotopic enrichment of leaf water as a result of the evaporative process of transpiration was first observed by Gonfiantini *et al.* (1965). In the same year, a model for predicting the isotopic enrichment that should take place at the surface of an evaporating body of water was published by Craig and Gordon (1965). This model can be applied to the isotopic composition of water at the evaporative sites within leaves (δ_e). Here, it is convenient to express the isotopic composition of the evaporative sites as enrichment in the heavier isotopes compared to source water, to account for the influence of different source-water isotopic signatures among plants. The enrichment of any plant water sample above source water (Δ_p) can be expressed as

$$\Delta_p = \frac{\delta_p - \delta_s}{1+\delta_s} \quad , \tag{2}$$

where δ_p is the δ value of the plant water sample and δ_s is that of source water. Here again, Δ_p, δ_p, and δ_s are often expressed as per mil. If this is the case, the δ_s in the denominator on the right side of the equation must be divided by 1000. A list of the main symbols and abbreviations used throughout the text is given in Table 1.

The Craig-Gordon model, as modified for application to leaves by subsequent authors (Dongmann *et al.* 1974; Flanagan, Comstock & Ehleringer 1991; Farquhar & Lloyd 1993), can be approximated by

$$\Delta_e \approx \varepsilon^+ + \varepsilon_k + (\Delta_v - \varepsilon_k)\frac{w_a}{w_i}, \tag{3}$$

where Δ_e is the enrichment of evaporative site water above source water, ε^+ is the equilibrium fractionation between liquid water and vapour, ε_k is the kinetic fractionation for combined diffusion through the stomata and the boundary layer, Δ_v is the isotopic enrichment of atmospheric vapour compared to source water, and w_a/w_i is the ratio of the water vapour mole fraction in the air relative to that in the intercellular air spaces. Thus, w_a/w_i is the relative humidity, but with the saturation water vapour mole fraction in the denominator calculated for leaf temperature rather than air temperature. If leaf temperature and air temperature are equal, w_a/w_i is exactly equal to the relative humidity of the air. The Δ_v is calculated with respect to source water as shown in Eqn 2, and it typically has a negative value due to the

equilibrium isotope effect between liquid and vapour. Equation 3 is a convenient approximation for the precise form of the model, as given by (Farquhar, Cernusak & Barnes 2007)

$$\Delta_e = (1+\varepsilon^+)\left[(1+\varepsilon_k)\left(1-\frac{w_a}{w_i}\right)+\frac{w_a}{w_i}(1+\Delta_v)\right]-1\,. \quad (4)$$

Note that in Eqn 3, the calculation can be readily performed with all isotopic terms expressed as per mil, whereas for Eqn 4, it is more straightforward to make the calculation with the isotopic terms not expressed as per mil, and then to multiply the result by 1000 afterward to return to per mil notation. In the supplementary material, we provide a Microsoft Excel spreadsheet with a combined data set of leaf water observations, which also contains a worked example of how to perform the calculation shown in Eqn 4. The difference between Δ_e calculated with Eqn 3 and that calculated with Eqn 4 is small for oxygen, on the order of 0.1‰. For hydrogen, it is larger, on the order of 1 to 2‰.

The equations shown above for predicting Δ_e assume isotopic steady state. Isotopic steady state means that the isotopic composition of the the transpired water vapour is equal to that of the source water supplying the leaf (Craig & Gordon 1965; Harwood *et al.* 1998; Farquhar & Cernusak 2005). The condition of non-steady state, when the transpired water has an isotopic composition differing from that of source water, will be discussed below. In general, it has been observed that leaf water enrichment tends to be near to steady state during the day in leaves that have relatively open stomata and do not show a high degree of succulence (Cernusak *et al.* 2008).

The equilibrium fractionation varies as a function of temperature (Bottinga & Craig 1969; Majoube 1971; Horita & Wesolowski 1994). It can be calculated according to the following equations (Majoube 1971), with that for ^{18}O shown first, followed by that for ^{2}H:

$$\varepsilon_O^+(‰) = \left[e^{\left(\frac{1.137}{(273+T)^2}\times 10^3-\frac{0.4156}{273+T}-2.0667\times 10^{-3}\right)}-1\right]\times 1000\,, \quad (5)$$

$$\varepsilon_H^+(‰) = \left[e^{\left(\frac{24.844}{(273+T)^2}\times 10^3-\frac{76.248}{273+T}+52.612\times 10^{-3}\right)}-1\right]\times 1000\,. \quad (6)$$

The right sides of the equations have been multiplied by 1000, so that ε^+ is here expressed as per mil. The symbol $\varepsilon_O^+(‰)$ in Eqn 5 refers to the isotope fractionation for ^{18}O, and $\varepsilon_H^+(‰)$ in Eqn 6 refers to that for ^{2}H. The *T* in these equations refers to the leaf temperature in degrees Celsius. The ε_k in Eqns 3 and 4 can be calculated as (Farquhar *et al.* 1989)

$$\varepsilon_k^O(‰) = \frac{28r_s+19r_b}{r_s+r_b}\,, \quad (7)$$

$$\varepsilon_k^H(‰) = \frac{25r_s+17r_b}{r_s+r_b}\,. \quad (8)$$

202 The ε_k^O (‰) is ε_k for ^{18}O expressed as per mil, and ε_k^H (‰) is the same for ^2H. The r_s and r_b
203 in Eqns 7 and 8 are the stomatal and boundary layer resistances, respectively (m^2 s mol^{-1});
204 they are the inverses of the stomatal and boundary layer conductances. The 28 and 19 in Eqn
205 7 are fractionation factors for diffusion of water molecules containing ^{18}O through the
206 stomata and boundary layer, expressed as per mil. The values 25 and 17 in Eqn 8 are those
207 same fractionation factors for ^2H (Merlivat 1978). It has been suggested that these values
208 should be revised (Cappa *et al.* 2003). However, subsequent measurements indicated that the
209 fractionation factors originally assigned are the more correct values (Luz *et al.* 2009).
210 If the water vapour in the air is in isotopic equilibrium with source water, then Δ_v will
211 approximately equal $-\varepsilon^+$. In that case, Eqn 3 will condense to
212 $$\Delta_e \approx (\varepsilon^+ + \varepsilon_k)\left(1 - \frac{w_a}{w_i}\right). \quad (9)$$
213 Equation 9 demonstrates the strong role that the relative humidity term w_a/w_i plays in
214 determining the isotopic enrichment of leaf water at the sites of evaporation.
215 Figure 3 shows the relationships between observed daytime bulk leaf water isotopic
216 enrichment and the air relative humidity and Craig-Gordon predictions for a large dataset
217 collected under natural field conditions across a sub-continental rainfall gradient in northern
218 Australia (Kahmen *et al.* 2013a). The analysis shows both the importance of the relative
219 humidity term in driving daytime leaf water stable isotope enrichment (Figures 3A and 3C),
220 and that the Craig-Gordon equation captures much of the observed variation across a large-
221 scale environmental gradient (Figures 3B and 3D).
222 This analysis also highlights an important difference between ^{18}O and ^2H. For ^{18}O,
223 the air relative humidity predicts nearly as much variation in the observed leaf water
224 enrichment as does the full Craig-Gordon model, with R^2 of 0.78 for the former versus 0.86
225 for the latter (Figures 3A and 3B). For ^2H, on the other hand, the air relative humidity
226 predicts only a little more than half the variation predicted by the full Craig-Gordon model,
227 with R^2 of 0.52 for the former versus 0.92 for the latter (Figures 3C and 3D). This
228 demonstrates the importance of the isotopic disequilibrium between air vapour and source
229 water for predicting Δ_e for ^2H in comparison to ^{18}O. This disequilibrium can be expressed as
230 $\varepsilon^+ + \Delta_v$. The contrast between ^2H and ^{18}O in the sensitivity of Δ_e to $\varepsilon^+ + \Delta_v$ comes about
231 because, for ^{18}O, ε^+, Δ_v, and the difference between them are typically small in absolute
232 value compared to ε_k, whereas the opposite is true for ^2H. For ^2H, the disequilibrium term
233 $\varepsilon^+ + \Delta_v$ can easily be larger than ε_k in absolute value, with either positive or negative values
234 possible. Thus, the predicted Δ_e for ^{18}O is dominated by the kinetic fractionation, ε_k; whereas

for ^2H, the predicted Δ_e is dominated by the equilibrium fractionation, ε^+, and by the air vapour disequilibrium term, $\varepsilon^+ + \Delta_v$.

The role of the atmospheric vapour isotopic composition in controlling Δ_e can be further appreciated by examining the limiting case where relative humidity is saturated, such that $w_a/w_i=1$. In this case, Eqn 3 reduces to $\varepsilon^+ + \Delta_v$; and, the isotopic disequilibrium between air vapour and source water then controls Δ_e. While this limiting scenario usually only occurs at night, it emphasises the importance of atmospheric vapour in influencing leaf water enrichment (Farquhar & Cernusak 2005; Helliker & Griffiths 2007), as well as the general importance of having a reasonably accurate estimate of Δ_v for predicting Δ_e, especially with respect to ^2H. In humid-zone epiphytes that use Crassulacean acid metabolism, this phenomenon creates an opportunity to reconstruct the isotope ratio of atmospheric water vapour from the epiphyte's organic matter (Helliker 2014).

Bulk leaf water

The term 'bulk leaf water' generally refers to a water sample obtained by extraction from a whole leaf. A bulk leaf water sample may or may not contain the water of the major veins, depending on the sampling protocol of the individual researcher. Leaf water excluding the major veins has also been referred to as 'lamina leaf water'. It is important to note that in the vast majority of plants, such a sample will also contain water associated with minor veins. Here we use δ_L to refer to the isotopic composition of bulk leaf water, and Δ_L to refer to its enrichment above source water.

Early measurements indicated that the Craig-Gordon model tended to overestimate Δ_L (Allison, Gat & Leaney 1985; Leaney *et al.* 1985; Bariac *et al.* 1989; Walker *et al.* 1989; Yakir, DeNiro & Gat 1990; Flanagan *et al.* 1991; Walker & Lance 1991). To illustrate this phenomenon, we compiled leaf water isotopic data from a number of published datasets, along with the Craig-Gordon prediction of leaf water enrichment corresponding to each observation (Supplementary material). The dataset contains 118 species, sampled across a range of tropical and temperate sites from both northern and southern hemispheres. It is limited to daytime observations of C_3 plants under natural field conditions. Figure 4 presents the results for the proportional difference between the predicted Craig-Gordon enrichment and the observed bulk leaf water enrichment ($1-\Delta_L/\Delta_e$). The analysis confirms that observed $1-\Delta_L/\Delta_e$ is larger than zero for both ^{18}O ($P<0.001$; $n=722$) and ^2H ($P<0.001$; $n=362$), with average proportional differences 0.12 for ^{18}O and 0.24 for ^2H.

The explanation for the generally lower observed value of Δ_L compared to Δ_e has attracted considerable research effort, because it is important to determine which leaf water signal is most relevant to the various applications that depend upon it. Two models have been proposed to explain this pattern when steady state conditions can reasonably be expected: a two-pools model, based on two discrete pools of water within the leaf, with one of them being unenriched xylem water (Leaney *et al.* 1985; Yakir, Deniro & Rundel 1989; Yakir *et al.* 1990; Roden & Ehleringer 1999; Song *et al.* 2015a); and an advection-diffusion, or Péclet, model (Farquhar & Lloyd 1993; Farquhar & Gan 2003; Barnes, Farquhar & Gan 2004).

If the two-pools model is assumed to comprise unenriched source water and enriched evaporative site water, it can be written as (Leaney *et al.* 1985; Song *et al.* 2015a)

$$\Delta_L = (1 - \phi)\Delta_e \,, \tag{10}$$

where ϕ is the proportion of leaf water that is unenriched xylem water, presumably residing mainly in the major veins and ground tissue associated with them. In this model, the overestimation of Δ_L by the Craig-Gordon model is due to the contribution from the unenriched pool.

Rather than two discrete pools, the Péclet model describes gradients of enrichment within the leaf water. In the Péclet model, advection of less enriched water by the transpiration stream opposes the back-diffusion of isotopically enriched water from the evaporative sites (Farquhar & Lloyd 1993). When advection overwhelms diffusion, the bulk leaf water enrichment will be less than that predicted by the Craig-Gordon equation. Accordingly, the proportional difference, $1-\Delta_L/\Delta_e$, is predicted to increase with increasing transpiration rate. This particular feature is an important distinction between the Péclet model and the two-pools model: the Péclet model predicts that the deviation of the bulk leaf water from the Craig-Gordon predicted enrichment should record information about the transpiration rate. In contrast, the two-pools model does not predict such an effect.

The Péclet number, which is dimensionless, represents the extent to which diffusion is overwhelmed by advective counter-flow (Ikeda 1983). It was originally developed to describe the ratio between convective and conductive heat transfer by Jean Claude Eugene Péclet, and has since been applied more generally to describe advection-diffusion effects on mass transport processes in permeable media. For leaves, the Péclet number, $\wp$, can be defined as vl/D, where v is the velocity of water movement (m s^{-1}), l is the distance (m) from the evaporative sites over which the Péclet effect is occurring, and D is the diffusivity of the

heavy isotopologue in water (m^2 s^{-1}). The D is temperature dependent, and can be modelled as a function of leaf temperature as (Cuntz *et al.* 2007),

$$D_O = 97.5 \times 10^{-9} e^{\left(-\frac{577}{T-145}\right)}, \quad (11)$$

$$D_H = 98.7 \times 10^{-9} e^{\left(-\frac{577}{T-145}\right)}, \quad (12)$$

where D_O is the diffusivity for $H_2{}^{18}O$, D_H is that for H^2HO, and T is leaf temperature in °C. The velocity of advection can further be described as kE/C, where E is the transpiration rate (mol m^{-2} s^{-1}), C is the molar concentration of water (5.55×10^4 mol m^{-3}), and k is a scaling factor to account for the tortuosity of the water path. The term E/C gives the velocity as if water were moving as a slab perpendicular to the leaf surface. The true velocity must be faster than the slab velocity, because water moves in a tortuous path through the leaf. The scaling factor k represents the ratio of the true velocity to the slab velocity. Combining the above terms gives the following definition for the Péclet number:

$$\wp = \frac{klE}{CD}. \quad (13)$$

It is convenient to combine k and l into a single term, which has been called the effective path length, L (Farquhar & Lloyd 1993):

$$\wp = \frac{LE}{CD}. \quad (14)$$

Ignoring the water in veins for the moment, the Péclet model applied to the average leaf lamina then predicts the following relationship with the evaporative site water enrichment (Farquhar & Lloyd 1993):

$$\Delta_L = \Delta_e \left(\frac{1-e^{-\wp}}{\wp}\right). \quad (15)$$

Equation 15 indicates that the smaller the Péclet number, the more similar Δ_L will be to Δ_e. It also predicts a continuous isotopic gradient from the sites of evaporation to the source water, modelled as an exponential decay along a cylindrical flow path.

Because $\wp$ includes terms for both the effective path length and the transpiration rate, a change in either one is predicted to alter the relationship between Δ_L and Δ_e. This is shown schematically in Figure 5. In practice, values for the effective path length L have been difficult to determine directly. Thus, they have generally been fitted using Eqns 14 and 15, which therefore involves comparing observed bulk leaf water enrichment with the predicted Craig-Gordon enrichment. One consideration that could lead to biased estimates of L when fitted in this way is that unenriched vein water could also contribute to the difference between Δ_L and Δ_e, as described by the two pool model. If this were the case, L would be overestimated if unenriched vein water were not accounted for prior to fitting Eqn 15.

Farquhar and Gan (2003) improved upon the one dimensional Péclet model described above by separating Péclet effects in the leaf xylem and lamina. In practical terms, this provides a means of combining the two-pool concept of dilution of leaf water enrichment by relatively unenriched vein water with the lamina Péclet model. Furthermore, it allows the advection-diffusion behaviour to be expressed in vein water as well as in mesophyll water. Such a consideration is important because some observations suggest that vein water can become enriched in ^{18}O (Gan *et al.* 2002; Gan *et al.* 2003). Farquhar and Gan (2003) suggested that most vein water should be found in the major veins and associated ground tissue, with the proportion of leaf water in higher order minor veins being relatively small. If the proportion of leaf water in minor veins were considered negligible, the bulk leaf water enrichment could then be described as (Farquhar & Gan 2003),

$$\Delta_L = \Delta_e \left[\phi_x e^{-\wp_r} + (1-\phi_x)\frac{1-e^{-\wp}}{\wp}\right], \quad (16)$$

where ϕ_x is the proportion of leaf water in major veins, and $\wp_r$ is the total radial Péclet number, equal to the sum of the lamina radial Péclet number, $\wp$, and the veinlet Péclet number, $\wp_{rv}$. Equation 16 allows for part of the difference between Δ_L and Δ_e to be accounted for by the relatively unenriched vein water. Fitting mesophyll effective path lengths with Eqn 16 should therefore provide more realistic estimates than with Eqn 15, but has the added complexity that values need to be assigned for ϕ_x and $\wp_r$ (e.g. Ripullone *et al.* 2008), or these need to be fitted simultaneously (e.g. Gan *et al.* 2003).

A convenient way to probe observed leaf water isotopic composition for evidence of Péclet effects is to plot the proportional difference between Δ_e and Δ_L as a function of transpiration rate. Such plots have yielded variable results, with some authors finding a positive relationship, as predicted by the Péclet model (Barbour *et al.* 2000b; Ripullone *et al.* 2008; Loucos *et al.* 2015), and others, either no detectable relationship or a negative relationship (Roden & Ehleringer 1999; Cernusak, Wong & Farquhar 2003; Song *et al.* 2013; Roden *et al.* 2015; Song *et al.* 2015a). For our combined dataset given in the supplementary material and shown in Figure 4, we find no relationship between $1-\Delta_L/\Delta_e$ and transpiration rate for either $\Delta^{18}O$ or $\Delta^{2}H$.

Given the conceptual realism in the Péclet model, it has been difficult to explain why in some cases there is no observable relationship between $1-\Delta_L/\Delta_e$ and E. One explanation might be changes in the effective path length as transpiration rate varies (Kahmen *et al.* 2008; Song *et al.* 2013; Loucos *et al.* 2015). Water supply to the mesophyll is predominantly via the minor veins (Sack & Holbrook 2006). Once in the mesophyll, water movement to the

sites of evaporation can proceed through three parallel pathways: symplastic movement through plasmodesmata, transcellular movement across cell membranes through aquaporins, and apoplastic flow in cell walls that are not suberised (Steudle, Murrmann & Peterson 1993). Although it can reasonably be expected that most flow will occur through the apoplast (Brodribb, Feild & Jordan 2007), each of these pathways is nonetheless likely to be associated with its own effective path length (Barbour & Farquhar 2004), and the possibility exists that the relative activity of these pathways may change with transpiration rate. In addition, water may not always evaporate in the vicinity of the stomatal pore (Rockwell, Holbrook & Stroock 2014; Buckley 2015), as is generally assumed. These considerations have potential to obscure the positive relationship between $1-\Delta_L/\Delta_e$ and E that is predicted by the Péclet model, because changes to L could compensate for changes in E, thereby decoupling $\wp$ from E (Cernusak & Kahmen 2013; Song *et al.* 2013).

The idea that xylem can be variably coupled to the mesophyll to give distinct pools of water of different volume and function within the leaf has been suggested in relation to leaf hydraulics (Zwieniecki, Brodribb & Holbrook 2007; Canny *et al.* 2012), and would support the idea of isotopic compartmentalisation of leaf water (Yakir *et al.* 1989; Yakir 1992; Yakir *et al.* 1994). Looking at the rehydration kinetics of leaves of different species, Zwieniecki *et al.* (2007) considered three observed patterns of hydraulic design: 1) where the vein is hydraulically separated from the rest of the leaf; 2) where the epidermis is hydraulically linked to the veins through the bundle sheath extension, but the mesophyll remains separated, and 3) where all tissues are equally well coupled (Figure 6). Such compartmentalisation could be created by both the internal organisation of leaf tissues, leading to variable degrees of physical contact between different structures, and by the number, activity, and resistance of the different pathways for water movement. A reasonable hypothesis, based on these observations, is that different residence times will occur for different pools of water within the leaf, introducing further variation into observed relationships between $1-\Delta_L/\Delta_e$ and E, because some pools of water would carry a memory of previous leaf water enrichment conditions, whereas others would not.

Conifer needles fit within Design 1 of Figure 6, consisting of a singular vascular bundle surrounded by transfusion tissue and a thick-walled endodermis, which likely provides high radial resistance and physical separation between xylem and mesophyll. Consistent with this concept, it was recently observed that a two-pool model was sufficient to explain the difference between the Craig-Gordon prediction and the observed bulk leaf water

enrichment in two pine species (Roden *et al.* 2015). Water pools may also exist within the mesophyll. In *Eucalyptus pauciflora* (snowgum) mesophyll cells shrank equally during transpiration (Canny & Huang 2006), whereas in *Gossypium hirsutum* (cotton), cavity and spongy mesophyll cells shrank more than matrix cells (Canny *et al.* 2012), suggesting that different pools of water differentially supported evaporative demand. Leaf shrinkage of tissues has also been linked more generally to the decline in extra-xylary hydraulic conductance (Scoffoni *et al.* 2014), which could further contribute to hydraulic compartmentalisation under conditions of water stress.

Progressive enrichment

Sampling leaf tissue at a sub-leaf scale has revealed spatial patterns of isotopic enrichment within leaves (Figure 7). Here, the isotopic composition tends to become progressively enriched towards the tip of the leaf and out from the mid-vein (Bariac *et al.* 1994; Wang & Yakir 1995; Helliker & Ehleringer 2000; Gan *et al.* 2002; Santrucek *et al.* 2007).

This spatial pattern was initially explained using a string of lakes model, which assumed a string of inter-connected pools of water within the leaf with differing isotope compositions (Gat & Bowser 1991; Helliker & Ehleringer 2000; Helliker & Ehleringer 2002). Farquhar and Gan (2003) improved upon this model by including Péclet effects in both mesophyll and veins (Figure 8). This enabled predictions of progressive enrichment of xylem water in monocot leaves with distance from the base of the leaf. The predictions matched relatively well the observed pattern in maize (Farquhar & Gan 2003; Gan *et al.* 2003). Ogée *et al.* (2007) then further improved upon this model by incorporating non-steady state effects.

The progressive enrichment observed in both monocot and dicot leaves suggests that back-diffusion occurs from the mesophyll back into the vein, allowing some evaporative enrichment to be passed via the xylem from central and basal portions of the leaf to downstream leaf sections. Such spatial variation can be described by three Péclet numbers (Figure 8): 1) a radial Péclet number at the interface between xylem and mesophyll ($\wp_{rv}$) which allows for the leaf veinlet xylem water to become enriched above petiole water; 2) a radial Péclet number associated with the mesophyll tissue ($\wp$) which is likely to be small; and 3) a longitudinal Péclet number ($\wp_l$), allowing progressive enrichment of the xylem in major veins in the direction of water movement, which is large, meaning mass transfer of

enrichment is mainly driven by advection. A derivation of this two dimensional Péclet model with component Péclet numbers is given by Farquhar & Gan (2003).

In a general sense, observations of progressive enrichment provide strong support for the concept of Péclet effects in leaf water, because increasing enrichment of vein water with increasing distance from the midrib and the leaf base would not occur if some enriched water did not back diffuse from the evaporative sites into the veins, against the advective flow of the vein water.

Transpired water

Water vapour leaving a leaf during transpiration originates directly from water at the evaporative sites. Thus, it makes intuitive sense that the isotopic composition of transpired water vapour (δ_E) should be related to that of evaporative site water (δ_e). When the Craig-Gordon model is written in a form that does not assume isotopic steady state, it predicts the following relationship between δ_e and δ_E:

$$\delta_e \approx \delta_E + \varepsilon^+ + \varepsilon_k + (\delta_v - \delta_E - \varepsilon_k)\frac{w_a}{w_i}. \quad (17)$$

From Eqn 17, it can be seen that δ_E is a necessary component for predicting δ_e under non-steady state conditions. When steady state is assumed, δ_E is set equal to δ_s. Making this substitution then leads to the widely used formulation shown in Eqn 3. If δ_E is measured experimentally, Eqn 17 provides a useful means of estimating the isotopic composition of the evaporative sites under non-steady state conditions (Harwood *et al.* 1998).

The steady-state assumption of δ_E being equal to δ_s results from mass balance constraints on leaf water dynamics, as shown in the following equation (Dongmann 1974; Farquhar & Cernusak 2005):

$$\frac{d(W\delta_L)}{dt} = E(\delta_s - \delta_E). \quad (18)$$

Here W is the leaf water concentration and δ_L is the isotope composition of leaf water. The product of the two is termed isostorage (Farquhar & Cernusak 2005). The term $E(\delta_s-\delta_E)$ describes the difference between the isotopic flux of water molecules into ($E\delta_s$) and out of ($E\delta_E$) the leaf, and thus can be viewed as the net isoflux. Equation 18 states that the rate of change of leaf water isostorage is equal to the net isoflux of water into or out of the leaf. With the leaf at isotopic steady state, leaf water isostorage would be constant (*i.e.*, $\frac{d(W\delta_L)}{dt} = 0$). Accordingly the net isoflux would be zero, such that δ_E must be equal to δ_s.

Motivated by the need to address the conditions under which isotopic steady state occurs (*i.e.*, $\delta_E=\delta_s$), several authors have used isotope ratio laser spectrometry coupled to a gas exchange system to explore the variability of δ_E in response to environmental conditions (Wang *et al.* 2012; Simonin *et al.* 2013; Dubbert *et al.* 2014; Song *et al.* 2015b). In a laboratory study conducted on tobacco and citrus leaves, Simonin et al. (2013) observed that δ_E was variable and deviated from δ_s as long as instability was present in any of the environmental and/or physiological variables (*e.g.*, relative humidity, δ_v, stomatal conductance). This suggests that environmental and physiological stability is a prerequisite for isotopic steady state to occur. In this context, it should be noted that even when environmental and physiological parameters are stable, the condition of isotopic steady state will not be achieved immediately (e.g. Simonin *et al.* 2013). Rather, δ_E will move toward δ_s in an exponential manner with a time constant that depends on the leaf water concentration, stomatal conductance, and the water vapour mole fraction inside the leaf (Dongmann *et al.* 1974; Farquhar & Cernusak 2005). Song *et al.* (2015b) recently conducted a laboratory experiment to monitor this type of exponential trajectory of δ_E in cotton leaves exposed to a gas-exchange cuvette environment. They demonstrated that the time constant for the approach of δ_E to δ_s agreed well with the prediction from the non-steady state isotope theory adapted to cuvette conditions.

Under field conditions, time constants for leaf water turnover can often be longer than the frequencies at which natural variations in temperature, humidity, and stomatal conductance occur. As a result, it has been argued that the isotopic composition of transpired water, δ_E, should rarely be precisely at steady state (Wang & Yakir 1995; Harwood *et al.* 1998; Simonin *et al.* 2013). A recent field study tracked diurnal variations in δ_E for an oak tree during distinct Mediterranean seasons and found that δ_E significantly deviated from δ_s most of the time (Dubbert *et al.* 2014). Such an observation, resulting from direct measurements of δ_E, provides support for the "steady state being rare" argument, thereby suggesting that the steady-state assumption should be used with caution in field conditions when applied to δ_E. However, this raises an interesting contrast with δ_L, the isotopic composition of leaf water, which often appears to be near to steady state, at least for many C_3 plants, during the day (*e.g.*, Figure 3). This highlights the difference between the isoflux ($E\delta_E$) and isostorage ($W\delta_L$) terms, with the latter being relatively buffered against high frequency variations.

Non-steady state effects on leaf water enrichment

Non-steady state effects on leaf water isotopic enrichment, the isostorage term, are expected to become important when stomatal conductance is low and/or when leaf water concentrations are high. Most species probably show significant non-steady state behaviour in Δ_L at night, due to low stomatal conductance (Cernusak, Pate & Farquhar 2002; Cernusak, Farquhar & Pate 2005; Seibt *et al.* 2006; Barnard *et al.* 2007; Cuntz *et al.* 2007). In addition, non-steady state behaviour has been observed during the day in plant species with succulent leaves (Sternberg, Deniro & Johnson 1986; Cernusak *et al.* 2008), and in some needle-leaved species, when exposed to high vapour pressure deficits or low soil water availability, such that stomatal conductance was relatively low (Pendall, Williams & Leavitt 2005; Seibt *et al.* 2006; Snyder *et al.* 2010).

Variation in leaf water isotopic enrichment under non-steady state conditions (Δ_{Ln}) can be predicted as follows (Farquhar & Cernusak 2005):

$$\Delta_{Ln} = \Delta_L - \frac{\alpha^+ \alpha_k}{g w_i} \cdot \frac{1 - e^{-\wp}}{\wp} \cdot \frac{d(W\Delta_{Ln})}{dt}, \quad (19)$$

where Δ_L is the steady-state prediction of leaf water isotopic enrichment, α^+ is defined as $1+\varepsilon^+$, α_k is defined as $1+\varepsilon_k$, W is the lamina leaf water concentration (mol m^{-2}), t is time (s), and g is the total conductance to water vapour of stomata plus boundary layer (mol m^{-2} s^{-1}). Note that ε^+ and ε_k, if they are expressed in per mil, should be divided by 1000 to calculate α^+ and α_k. Equation 19 has the term Δ_{Ln} on both the left and right sides of the equation, and so needs to be solved iteratively. One way to do this is with the Solver function in Microsoft Excel (Farquhar & Cernusak 2005). Alternatively, Kahmen et al. (2008) suggested a simpler method for solving the equation by introducing the assumption that, over sufficiently small time steps, $\frac{d(W\Delta_{Ln})}{dt} \approx \frac{W\Delta_{Ln} - (W\Delta_{Ln})_{t-1}}{\Delta_t}$, where the subscript t-1 refers to the value at the previous time step and Δ_t is the time elapsed since the previous time step. This definition can be substituted into Eqn 19, which can then be solved for Δ_{Ln}, such that it only occurs on the left side of the equation. The value for Δ_{Ln} can then be calculated without need for iteration (Kahmen *et al.* 2008). Another alternative is to assume a step change in parameters from one time step to the next, so that the leaf water enrichment moves toward the new steady state in an exponential fashion with a time constant, τ, approximated by W/gw_i. This also results in equations that can be calculated without need for iteration (Dongmann *et al.* 1974; Farquhar & Cernusak 2005; Cuntz *et al.* 2007).

Which leaf water model to use?

As seen above, models describing leaf water evaporative enrichment have become increasingly complex over time, from the simplest version of the Craig-Gordon equation, to non-steady state models (Dongmann *et al.* 1974; Farquhar & Cernusak 2005), to the most complex spatially-explicit models describing gradients of enrichment under non-steady state conditions (Cuntz *et al.* 2007; Ogée *et al.* 2007). Given the range of options available, it is not always straight forward to decide which leaf water model to use for a particular research question. For some applications at larger temporal and spatial scales, the steady state Craig-Gordon model (Eqn 3) will be adequate and including non-steady state effects and Péclet effects will likely add complexity that does not significantly improve model outcomes. Conversely, if water is sampled within a leaf and at high temporal resolution, a spatially-explicit and non-steady state model may be required (Ogée *et al.* 2007). Some studies have tested the suitability of different models in specific applications. For example, Cernusak et al. (2005) demonstrated that both the non-steady state and whole-leaf Péclet models were required to predict accurately diel variability in leaf water enrichment in *Eucalyptus globulus.* Ogée et al. (2009) found that the oxygen isotope composition of tree ring cellulose was not sensitive to the value assigned to the Péclet effective length, implying that a simpler two-pool model would have been adequate. At larger spatial but smaller temporal scale, the requirement for a non-steady state model has been confirmed when interpreting variation in ecosystem-scale isofluxes (Xiao *et al.* 2012; Santos *et al.* 2014).

Here, we describe a general framework for deciding when to apply different leaf water models. Questions relating to the $\delta^{18}O$ of oxygen evolution, such as studies of the Earth's Dole effect (Bender, Sowers & Labeyrie 1994; Hoffmann *et al.* 2004), should for the most part be well served by the steady state Craig-Gordon prediction of Δ_e. This is because oxygen evolution takes place during the day when leaf water is generally near isotopic steady state, and because chloroplasts are mostly located near to the evaporative sites. The same argument can be applied for questions relating to effects of photosynthesis on $\delta^{18}O$ of atmospheric CO_2 (Farquhar *et al.* 1993; Cuntz *et al.* 2003). However, in this case the impact of exchange of atmospheric CO_2 with leaf water also continues at night. In order to account for the influence of dark respiration on $\delta^{18}O$ of atmospheric CO_2, a non-steady state model of evaporative site water is needed (Cernusak *et al.* 2004; Seibt *et al.* 2006; Cuntz *et al.* 2007; Santos *et al.* 2014).

For the most part, the influence of leaf water isotopic enrichment on organic material is mediated by photosynthesis. Again, because photosynthesis takes place during the day, research questions relating to $\delta^{18}O$ and $\delta^{2}H$ of organic material should be served reasonably well by steady state models. Here, there have been mixed results as to whether Péclet effects need to be considered. For isotopic signals closely related to leaf water, such as $\delta^{18}O$ of phloem sugars, a Péclet effect was required (Barbour *et al.* 2000b; Cernusak *et al.* 2003). However, in applications that consider processes further downstream from leaf water, such as tree-ring formation, the relatively small Péclet effect becomes further damped, to the point that there may be little advantage in including it (Ogée *et al.* 2009; Gessler *et al.* 2014; Song, Clark & Helliker 2014).

For plant breeding applications aimed at disentangling effects of stomatal conductance from those of photosynthetic capacity on water-use efficiency, it will likely be advantageous to consider Péclet effects (Farquhar, Condon & Masle 1994; Barbour *et al.* 2000a; Barbour 2007). In addition, Péclet effects will likely be particularly important in studies aimed at linking leaf water stable isotope composition with leaf hydraulic pathways (Barbour & Farquhar 2004; Ferrio *et al.* 2012; Song *et al.* 2013). On the other hand, for applications aimed at using the $\delta^{2}H$ of leaf waxes to reconstruct hydrological features of ancient ecosystems, the simplest form of the steady state Craig-Gordon equation will likely suffice (McInerney, Helliker & Freeman 2011; Sachse *et al.* 2012; Kahmen *et al.* 2013a).

SAMPLING CONSIDERATIONS AND METHODOLOGICAL ADVANCES

The isotopic analysis of plant waters presents a number of analytical challenges. These include difficulties of extraction, the necessity to work with small quantities of water, protecting the original composition of the water sample, and avoiding undesirable influences of dissolved compounds. Preventing post-sampling evaporative enrichment of leaf water requires careful consideration of sample handling and storage. For example, even the time taken to separate primary veins from leaf lamina can result in detectable isotopic enrichment of the leaf lamina (Cernusak *et al.* 2003).

There are three main ways of analysing the isotopic composition of plant water: equilibration, prior extraction, and simultaneous extraction. With equilibration methods, a gas is equilibrated directly with the plant water while it is still in the sample, and the gas is then analysed for its isotopic composition. With prior extraction, the water is taken out of the

plant tissue before isotopic analysis, whereas with simultaneous extraction the water is removed from the plant as part of the analysis.

In equilibration methods, a gas is introduced into a sealed vessel with the sample, such as a detached portion of stem, and the system maintained until the gas has effectively equilibrated with the water that the sample contains (Scrimgeour 1995). Typically, for oxygen isotopic analysis, pure CO_2 or a CO_2/gas mixture is stored over the sample at a controlled temperature. The CO_2 then exchanges oxygen with the water by the carbonic acid/bicarbonate reaction, with a temperature dependent fractionation. Direct equilibration of CO_2 with twig and stem water showed good agreement, to within 0.5‰, with assessments of the $\delta^{18}O$ of paired samples based on prior extraction (Scrimgeour 1995). This direct equilibration method may also be useful for analysis of the $\delta^{18}O$ of leaf water. However, a limitation may be imposed by the very low rate of diffusion of CO_2 in water, and of water in water, so that the gas may primarily equilibrate with the more exposed portion of the leaf water. Thus, the $\delta^{18}O$ of the equilibrated CO_2 may be more representative of the evaporative site water, as opposed to the bulk leaf water; experiments are needed to test this.

Extraction methods aim for complete removal of the water from the sample, because the removal of water by evaporation is typically associated with a fractionation. Thus, in the event of a partial extraction, the water removed will have a different isotopic composition from that which remains. The most widely used prior extraction method is cryogenic vacuum extraction (Ehleringer, Roden & Dawson 2000). Here, the water is freed from the sample using heat and vacuum, and then frozen onto a collecting surface. For plant tissues, cryogenic vacuum extraction is a tested and reliable method, and it typically serves as the benchmark against which new methods are evaluated. However, it is relatively labour and time-intensive. Several authors have proposed modifications aimed at reducing these restrictions (West, Patrickson & Ehleringer 2006a; Vendramini & Sternberg 2007; Koeniger *et al.* 2011; Ignatev *et al.* 2013; Orlowski *et al.* 2013). For laser-based analysis of water isotopes, cryogenic extraction also presents the challenge of transferring organic contaminants that can mix with the water sample and cause optical interference (West *et al.* 2010).

Recent years have seen the advent of laser-based, optical analysers with the capacity to measure the stable isotope composition of water vapour (e.g. Gupta *et al.* 2009; Sturm & Knohl 2010; Aemisegger *et al.* 2012; Griffis 2013). Using this type of analyser, new methods have been developed for simultaneous water extraction and analysis. Here, the leaf

625 is placed in the extraction device and the resulting water vapour is analysed as it is driven off
626 by heating. One example of such a system is an induction module cavity ring down
627 spectroscopy system (IM-CRDS) (Berkelhammer *et al.* 2013). The laser isotope analyser
628 relies on the absorption of an infrared laser pulse by water vapour as it reflects inside a
629 chamber. For a typical liquid water injection, about 1 µL of water is vaporised when it is
630 injected into a chamber hotter than boiling point. The vapour is then carried into the analyser
631 in a non-interfering gas. The IM-CRDS system is similar, except that the leaf sample is
632 heated inductively, and the vapour produced is then carried into the laser analyser. A second
633 example of a simultaneous water extraction and analysis system uses a microwave oven to
634 heat the leaf sample (Munksgaard *et al.* 2014). This was termed ME-IRIS, for microwave
635 extraction isotope ratio infrared spectroscopy. The ME-IRIS system includes a microwave
636 and a condenser to moderate the water vapour concentration of air passing to the laser
637 analyser, so that it remains within the optimal measuring range. Advantages of ME-IRIS are
638 that it can handle larger samples (*e.g.*, whole leaves), and that it uses relatively low cost
639 components, such as a domestic microwave oven.
640 A complication in these simultaneous extraction methods is that some organic
641 compounds, for example alcohols, which can be present in leaf water, interfere significantly
642 with absorption peaks for the target isotopologues in the laser analyser. Two solutions have
643 been developed: a small furnace in-line which breaks down the interfering compounds, and
644 post-processing software that detects and flags analyses that potentially contain spectral
645 interference. The combination of the two tools together appears sufficient to identify and/or
646 reduce the analytical errors associated with organic contaminants to acceptable levels (West
647 *et al.* 2011; Munksgaard *et al.* 2014; Martín-Gómez *et al.* 2015).
648 Both IM-CRDS and ME-IRIS also suffer from memory effects, often requiring two to
649 three sample analyses to overcome the influence of a previous sample if its isotopic
650 composition was substantially different (Berkelhammer *et al.* 2013; Munksgaard *et al.* 2014).
651 The impact of the memory effect can be minimized by arranging the analytical sequence in
652 such a way as to avoid large jumps in isotopic composition between adjacent samples. This
653 also highlights a further disadvantage of simultaneous extraction methods; once analysed, the
654 same sample is not available for re-analysis. Thus, wherever possible, samples should be
655 collected in sufficient replication to overcome memory effects and as back-up in the event
656 that a re-analysis is deemed necessary. The main advantage gained by simultaneous
657 extraction is the capacity to analyse samples in the field at the study site or in a temporary

658 field laboratory, and to thereby have analytical results in near real time so that they can
659 inform the proceeding sampling strategy and experimental design.
660 An interesting variant of an equilibration method and simultaneous analysis of water
661 vapour stable isotopes by a laser analyser has been applied to soil cores (Wassenaar *et al.*
662 2008). In this system, a soil core was placed inside a sealed, inflatable plastic bag. The
663 sealed bag was then left to equilibrate the water vapour in the headspace with the liquid water
664 in the soil sample. Following the appropriate equilibration time, the plastic bag was
665 punctured with a needle connected to a piece of tubing feeding directly into a laser analyser.
666 The $\delta^{18}O$ and $\delta^{2}H$ of the liquid water in the soil sample could then be inferred from the
667 temperature dependent equilibrium fractionation between liquid and vapour, ε^{+}. Such a
668 system may also be suitable for plant materials. Advantages would be the simplicity of the
669 equilibration compared to liquid water extraction, and that isotope ratios of both oxygen and
670 hydrogen could be determined simultaneously. As with the direct equilibration of CO_2, a
671 question that would need to be addressed for leaves is whether the water vapour in the
672 headspace primarily equilibrates with the evaporative site, or whether it equilibrates with the
673 bulk leaf water.
674

675 **CONCLUSIONS**

676 Steady state leaf water isotopic enrichment is closely related to relative humidity in
677 natural environments, with the observed enrichment decreasing with increasing relative
678 humidity. Isotopic disequilibrium between source water and atmospheric vapour can also
679 have a relatively strong effect on steady state leaf water isotopic composition. Observations
680 over a large scale environmental gradient in Australia indicated that this effect is likely to be
681 stronger for ^{2}H than for ^{18}O. This difference in behaviour between the two isotopes reflects
682 the relative magnitudes of the equilibrium and kinetic fractionations in the Craig-Gordon
683 model of evaporative site enrichment. Equilibrium effects dominate for ^{2}H, whereas kinetic
684 effects dominate for ^{18}O.
685 In a combined dataset including 118 species, we found that observed bulk leaf water
686 was less enriched than the Craig-Gordon predictions for both ^{18}O and ^{2}H, as has been shown
687 previously. Across the full dataset, the proportional difference between Craig-Gordon
688 predicted and observed bulk leaf water enrichment showed no relationship with transpiration
689 rate. Explaining why Péclet effects are detectable in some situations, but not in others,
690 remains a challenge. Linking observed patterns of leaf water isotopic enrichment with

specific hydraulic characteristics could provide a tractable way forward, especially with respect to pathways for water movement from veins to evaporative sites.

The development of new technologies for quantifying stable isotope ratios of transpired water and water extracted from plant tissues offers an opportunity to further our understanding of the finer scale controls over leaf water stable isotope enrichment. For example, measuring the isotopic composition of transpired water vapour provides a means of detecting nuances of steady versus non-steady state behaviour, and it also has potential to provide insight into whether slow turnover pools exist within the leaf water, indicative of hydraulic compartmentalisation. Improving our understanding of the environmental and physiological controls over leaf water stable isotopic enrichment will benefit the many applications to which models of this process can be applied, and may additionally lead to novel insights into hydraulic design and functioning in leaves of terrestrial plants.

ACKNOWLEDGMENTS

This review paper resulted from a workshop funded by James Cook University and held at the Daintree Rainforest Observatory in September 2014. L.A.C. and F.A.M. were supported by Australian Research Council Future Fellowships (FT100100329 and FT110100793, respectively). N.B.E. was supported by an Australian Research Council Discovery Early Career Researcher Award (DE130100295).

REFERENCES

Aemisegger F., Sturm P., Graf P., Sodemann H., Pfahl S., Knohl A. & Wernli H. (2012) Measuring variations of $\delta^{18}O$ and $\delta^{2}H$ in atmospheric water vapour using two commercial laser-based spectrometers: an instrument characterisation study. *Atmospheric Measurement Techniques* **5**, 1491-1511.

Allison G.B., Barnes C.J. & Hughes M.W. (1983) The distribution of deuterium and ^{18}O on dry soils. 2. Experimental. *Journal of Hydrology* **64**, 377-397.

Allison G.B., Gat J.R. & Leaney F.W.J. (1985) The relationship between deuterium and oxygen-18 delta values in leaf water. *Chemical Geology* **58**, 145-156.

Araguas-Araguas L., Froehlich K. & Rozanski K. (2000) Deuterium and oxygen-18 isotope composition of precipitation and atmospheric moisture. *Hydrological Processes* **14**, 1341-1355.

723 Barbour M.M. (2007) Stable oxygen isotope composition of plant tissue: a review.
724 *Functional Plant Biology* **34**, 83-94.
725 Barbour M.M. & Farquhar G.D. (2004) Do pathways of water movement and leaf anatomical
726 dimensions allow development of gradients in $H_2{}^{18}O$ between veins and the sites of
727 evaporation within leaves? *Plant Cell and Environment* **27**, 107-121.
728 Barbour M.M., Fischer R.A., Sayre K.D. & Farquhar G.D. (2000a) Oxygen isotope ratio of
729 leaf and grain material correlates with stomatal conductance and grain yield in
730 irrigated wheat. *Australian Journal of Plant Physiology* **27**, 625-637.
731 Barbour M.M., Schurr U., Henry B.K., Wong S.-C. & Farquhar G.D. (2000b) Variation in the
732 oxygen isotope ratio of phloem sap sucrose from castor bean. Evidence in support of
733 the Péclet effect. *Plant Physiology* **123**, 671-679.
734 Bariac T., Gonzalezdunia J., Tardieu F., Tessier D. & Mariotti A. (1994) Spatial variation of
735 the isotopic composition of water (^{18}O, ^{2}H) in organs of aerophytic plants: 1.
736 Assessment under laboratory conditions. *Chemical Geology* **115**, 307-315.
737 Bariac T., Rambal S., Jusserand C. & Berger A. (1989) Evaluating water fluxes of field-
738 grown alfalfa from diurnal observations of natural isotope concentrations, energy
739 budget and ecophysiological parameters. *Agricultural and Forest Meteorology* **48**,
740 263-283.
741 Barnard R.L., Salmon Y., Kodama N., Sorgel K., Holst J., Rennenberg H., Gessler A. &
742 Buchmann N. (2007) Evaporative enrichment and time lags between $\delta^{18}O$ of leaf
743 water and organic pools in a pine stand. *Plant Cell and Environment* **30**, 539-550.
744 Barnes B., Farquhar G. & Gan K. (2004) Modelling the isotope enrichment of leaf water.
745 *Journal of Mathematical Biology* **48**, 672-702.
746 Barnes C.J. & Allison G.B. (1983) The distribution of deuterium and ^{18}O in dry soils. 1.
747 Theory. *Journal of Hydrology* **60**, 141-156.
748 Bender M., Sowers T. & Labeyrie L. (1994) The Dole effect and its variations during the last
749 130,000 years as measured in the Vostok ice core. *Global Biogeochemical Cycles* **8**,
750 363-376.
751 Berkelhammer M., Hu J., Bailey A., Noone D.C., Still C.J., Barnard H., Gochis D., Hsiao
752 G.S., Rahn T. & Turnipseed A. (2013) The nocturnal water cycle in an open-canopy
753 forest. *Journal of Geophysical Research: Atmospheres* **118**, 10,225-210,242.

754 Bottinga Y. & Craig H. (1969) Oxygen isotope fractionation between CO_2 and water, and the
755 isotopic composition of marine atmospheric CO_2. *Earth and Planetary Science*
756 *Letters* **5**, 285-295.
757 Bowen G.J. (2010) Isoscapes: spatial pattern in isotopic biogeochemistry. *Annual Review of*
758 *Earth and Planetary Sciences* **38**, 161-187.
759 Brodribb T.J., Feild T.S. & Jordan G.J. (2007) Leaf maximum photosynthetic rate and
760 venation are linked by hydraulics. *Plant Physiology* **144**, 1890-1898.
761 Brooks J.R., Barnard H.R., Coulombe R. & McDonnell J.J. (2010) Ecohydrologic separation
762 of water between trees and streams in a Mediterranean climate. *Nature Geoscience* **3**,
763 100-104.
764 Buckley T.N. (2015) The contributions of apoplastic, symplastic and gas phase pathways for
765 water transport outside the bundle sheath in leaves. *Plant Cell and Environment* **38**, 7-
766 22.
767 Canny M., Wong S.C., Huang C. & Miller C. (2012) Differential shrinkage of mesophyll
768 cells in transpiring cotton leaves: implications for static and dynamic pools of water,
769 and for water transport pathways. *Functional Plant Biology* **39**, 91-102.
770 Canny M.J. & Huang C.X. (2006) Leaf water content and palisade cell size. *New Phytologist*
771 **170**, 75-85.
772 Cappa C.D., Hendricks M.B., DePaulo D.J. & Cohen R.C. (2003) Isotopic fractionation of
773 water during evaporation. *Journal of Geophysical Research* **108**, 4525.
774 Cernusak L.A., Farquhar G.D. & Pate J. (2005) Environmental and physiological controls
775 over oxygen and carbon isotope composition of Tasmanian blue gum, *Eucalyptus*
776 *globulus*. *Tree Physiology* **25**, 129-146.
777 Cernusak L.A., Farquhar G.D., Wong S.C. & Stuart-Williams H. (2004) Measurement and
778 interpretation of the oxygen isotope composition of carbon dioxide respired by leaves
779 in the dark. *Plant Physiology* **136**, 3350-3363.
780 Cernusak L.A. & Kahmen A. (2013) The multifaceted relationship between leaf water 18O
781 enrichment and transpiration rate. *Plant Cell and Environment* **36**, 1239-1241.
782 Cernusak L.A., Mejia-Chang M., Winter K. & Griffiths H. (2008) Oxygen isotope
783 composition of CAM and C_3 *Clusia* species: non-steady-state dynamics control leaf
784 water ^{18}O enrichment in succulent leaves. *Plant Cell and Environment* **31**, 1644-1662.
785 Cernusak L.A., Pate J.S. & Farquhar G.D. (2002) Diurnal variation in the stable isotope
786 composition of water and dry matter in fruiting *Lupinus angustifolius* under field
787 conditions. *Plant, Cell & Environment* **25**, 893-907.

788 Cernusak L.A., Wong S.-C. & Farquhar G.D. (2003) Oxygen isotope composition of phloem
789 sap in relation to leaf water in *Ricinus communis*. *Functional Plant Biology* **30**, 1059-
790 1070.
791 Coplen T.B. (2011) Guidelines and recommended terms for expression of stable-isotope-ratio
792 and gas-ratio measurement results. *Rapid Communications in Mass Spectrometry* **25**,
793 2538-2560.
794 Craig H. & Gordon L.I. (1965) Deuterium and oxygen-18 variations in the ocean and the
795 marine atmosphere. In: *Proceedings of a conference on stable isotopes in*
796 *oceanographic studies and palaeotemperatures* (ed E. Tongiorgi), pp. 9-130. Lischi
797 and Figli, Pisa.
798 Cuntz M., Ciais P., Hoffmann G. & Knorr W. (2003) A comprehensive global three-
799 dimensional model of $\delta^{18}O$ in atmospheric CO_2: 1. Validation of surface processes.
800 *Journal of Geophysical Research* **108**, 4527.
801 Cuntz M., Ogée J., Farquhar G.D., Peylin P. & Cernusak L.A. (2007) Modelling advection
802 and diffusion of water isotopologues in leaves. *Plant, Cell and Environment* **30**, 892-
803 909.
804 Dawson T.E. (1993) Water sources of plants as determined from xylem-water isotopic
805 composition: perspectives on plant competition, distribution, and water relations. In:
806 *Stable isotopes and plant carbon-water relations* (eds J.R. Ehleringer, A.E. Hall, &
807 G.D. Farquhar), pp. 465-496. Academic Press Inc., San Diego.
808 Dawson T.E., Mambelli S., Plamboeck A.H., Templer P.H. & Tu K.P. (2002) Stable isotopes
809 in plant ecology. *Annual Review of Ecology and Systematics* **33**, 507-559.
810 Dole M., Lane G.A., Rudd D.P. & Zaukelies D.A. (1954) Isotopic composition of
811 atmospheric oxygen and nitrogen. *Geochimica et Cosmochimica Acta* **6**, 65-78.
812 Dongmann G., Nurnberg H.W., Förstel H. & Wagener K. (1974) On the enrichment of $H_2{}^{18}O$
813 in the leaves of transpiring plants. *Radiation and Environmental Biophysics* **11**, 41-52.
814 Dubbert M., Cuntz M., Piayda A. & Werner C. (2014) Oxygen isotope signatures of
815 transpired water vapor: the role of isotopic non-steady-state transpiration under
816 natural conditions. *New Phytologist* **203**, 1242-1252.
817 Eglinton T.I. & Eglinton G. (2008) Molecular proxies for paleoclimatology. *Earth and*
818 *Planetary Science Letters* **275**, 1-16.
819 Ehleringer J.R. & Dawson T.E. (1992) Water-uptake by plants - perspectives from stable
820 isotope composition. *Plant Cell and Environment* **15**, 1073-1082.

821 Ehleringer J.R., Roden J.S. & Dawson T.E. (2000) Asessing ecosystem-level water relations
822 through stable isotope ratio analyses. In: *Methods in Ecosystem Science* (eds O.E.
823 Sala, R.B. Jackson, H.A. Mooney, & R.W. Howarth), pp. 181-198. Springer-Verlag,
824 New York.
825 Ellsworth P.Z. & Williams D.G. (2007) Hydrogen isotope fractionation during water uptake
826 by woody xerophytes. *Plant and Soil* **291**, 93-107.
827 English N.B., Dettman D.L., Sandquist D.R. & Williams D.G. (2007) Past climate changes
828 and ecophysiological responses recorded in the isotope ratios of saguaro cactus
829 spines. *Oecologia* **154**, 247-258.
830 Farquhar G.D. & Cernusak L.A. (2005) On the isotopic composition of leaf water in the non-
831 steady state. *Functional Plant Biology* **32**, 293-303.
832 Farquhar G.D., Cernusak L.A. & Barnes B. (2007) Heavy water fractionation during
833 transpiration. *Plant Physiology* **143**, 11-18.
834 Farquhar G.D., Condon A.G. & Masle J. (1994) Use of carbon and oxygen isotope
835 composition and mineral ash content in breeding for improved rice production under
836 favorable, irrigated conditions. In: *Breaking the yield barrier* (ed K.G. Cassman), pp.
837 95-101. International Rice Research Institute, Manila.
838 Farquhar G.D. & Gan K.S. (2003) On the progressive enrichment of the oxygen isotopic
839 composition of water along leaves. *Plant, Cell and Environment* **26**, 801-819.
840 Farquhar G.D., Hubick K.T., Condon A.G. & Richards R.A. (1989) Carbon isotope
841 fractionation and plant water-use efficiency. In: *Stable isotopes in ecological research*
842 (eds P.W. Rundel, J.R. Ehleringer, & K.A. Nagy), pp. 21-46. Springer-Verlag, New
843 York.
844 Farquhar G.D. & Lloyd J. (1993) Carbon and oxygen isotope effects in the exchange of
845 carbon dioxide between terrestrial plants and the atmosphere. In: *Stable isotopes and*
846 *plant carbon-water relations* (eds J.R. Ehleringer, A.E. Hall, & G.D. Farquhar), pp.
847 47-70. Academic Press, San Diego.
848 Farquhar G.D., Lloyd J., Taylor J.A., Flanagan L.B., Syvertsen J.P., Hubick K.T., Wong S.C.
849 & Ehleringer J.R. (1993) Vegetation effects on the isotope composition of oxygen in
850 atmospheric CO_2. *Nature* **363**, 439-443.
851 Ferrio J.P., Pou A., Florez-Sarasa I., Gessler A., Kodama N., Flexas J. & Ribas-Carbo M.
852 (2012) The Péclet effect on leaf water enrichment correlates with leaf hydraulic
853 conductance and mesophyll conductance for CO_2. *Plant Cell and Environment* **35**,
854 611-625.

855 Flanagan L.B., Comstock J.P. & Ehleringer J.R. (1991) Comparison of modeled and
856 observed environmental influences on the stable oxygen and hydrogen isotope
857 composition of leaf water in *Phaseolis vulgaris* L. *Plant Physiology* **96**, 588-596.
858 Gan K.S., Wong S.C., Yong J.W.H. & Farquhar G.D. (2002) ^{18}O spatial patterns of vein
859 xylem water, leaf water, and dry matter in cotton leaves. *Plant Physiology* **130**, 1008-
860 1021.
861 Gan K.S., Wong S.C., Yong J.W.H. & Farquhar G.D. (2003) Evaluation of models of leaf
862 water ^{18}O enrichment using measurements of spatial patterns of vein xylem water,
863 leaf water and dry matter in maize leaves. *Plant Cell and Environment* **26**, 1479-1495.
864 Gat J.R. & Bowser C. (1991) The heavy isotope enrichment of water in coupled evaporative
865 systems. In: *Stable Isotope Geochemistry: A Tribute to Samuel Epstein* (eds H.P.
866 Taylor, J.R. O'Neil, & I.R. Kaplan), pp. 159-168. The Geochemical Society, St.
867 Louis.
868 Gedzelman S.D. & Arnold R. (1994) Modeling the isotopic composition of precipitation.
869 *Journal of Geophysical Research-Atmospheres* **99**, 10455-10471.
870 Gessler A., Ferrio J.P., Hommel R., Treydte K., Werner R.A. & Monson R.K. (2014) Stable
871 isotopes in tree rings: towards a mechanistic understanding of isotope fractionation
872 and mixing processes from the leaves to the wood. *Tree Physiology* **34**, 796-818.
873 Gonfiantini R., Gratziu S. & Tongiorgi E. (1965) Oxygen isotope composition of water in
874 leaves. In: *Isotopes and radiation in soil-plant nutrition studies*, pp. 405-410. IAEA,
875 Vienna.
876 Griffis T.J. (2013) Tracing the flow of carbon dioxide and water vapor between the biosphere
877 and atmosphere: A review of optical isotope techniques and their application.
878 *Agricultural and Forest Meteorology* **174**, 85-109.
879 Gupta P., Noone D., Galewsky J., Sweeney C. & Vaughn B.H. (2009) Demonstration of
880 high-precision continuous measurements of water vapor isotopologues in laboratory
881 and remote field deployments using wavelength-scanned cavity ring-down
882 spectroscopy (WS-CRDS) technology. *Rapid Communications in Mass Spectrometry*
883 **23**, 2534-2542.
884 Harwood K.G., Gillon J.S., Griffiths H. & Broadmeadow M.S.J. (1998) Diurnal variation of
885 $\Delta^{13}CO_2$, $\Delta C^{18}O^{16}O$, and evaporative site enrichment of $\delta H_2{}^{18}O$ in *Piper aduncum*
886 under field conditions in Trinidad. *Plant, Cell & Environment* **21**, 269-283.

887 Helliker B.R. (2014) Reconstructing the $\delta^{18}O$ of atmospheric water vapour via the CAM
888 epiphyte *Tillandsia usneoides*: seasonal controls on $\delta^{18}O$ in the field and large-scale
889 reconstruction of $\delta^{18}O_a$. *Plant Cell and Environment* **37**, 541-556.
890 Helliker B.R. & Ehleringer J.R. (2000) Establishing a grassland signature in veins: ^{18}O in the
891 leaf water of C_3 and C_4 grasses. *Proceedings of the National Academy of Sciences* **97**,
892 7894-7898.
893 Helliker B.R. & Ehleringer J.R. (2002) Differential ^{18}O enrichment of leaf cellulose in C_3
894 versus C_4 grasses. *Functional Plant Biology* **29**, 435-442.
895 Helliker B.R. & Griffiths H. (2007) Toward a plant-based proxy for the isotope ratio of
896 atmospheric water vapor. *Global Change Biology* **13**, 723-733.
897 Hoffmann G., Cuntz M., Weber C., Ciais P., Friedlingstein P., Heimann M., Jouzel J., Kaduk
898 J., Maier-Reimer E., Seibt U. & Six K. (2004) A model of the Earth's Dole effect.
899 *Global Biogeochemical Cycles* **18**, 1008.
900 Horita J. & Wesolowski D.J. (1994) Liquid-vapor fractionation of oxygen and hydrogen
901 isotopes of water from the freezing to the critical temperature. *Geochimica Et*
902 *Cosmochimica Acta* **58**, 3425-3437.
903 IAEA/WMO (2011) Global Network of Isotopes in Precipitation. The GNIP Database. .
904 Ignatev A., Velivetckaia T., Sugimoto A. & Ueta A. (2013) A soil water distillation technique
905 using He-purging for stable isotope analysis. *Journal of Hydrology* **498**, 265-273.
906 Ikeda T. (1983) *Maximum principle in finite element models for convection-diffusion*
907 *phenomena*. North Holland, Amsterdam.
908 Kahmen A., Hoffmann B., Schefuss E., Arndt S.K., Cernusak L.A., West J.B. & Sachse D.
909 (2013a) Leaf water deuterium enrichment shapes leaf wax n-alkane δD values of
910 angiosperm plants II: Observational evidence and global implications. *Geochimica Et*
911 *Cosmochimica Acta* **111**, 50-63.
912 Kahmen A., Sachse D., Arndt S.K., Tu K.P., Farrington H., Vitousek P.M. & Dawson T.E.
913 (2011) Cellulose $\delta^{18}O$ is an index of leaf-to-air vapor pressure difference (VPD) in
914 tropical plants. *Proceedings of the National Academy of Sciences of the United States*
915 *of America* **108**, 1981-1986.
916 Kahmen A., Schefuss E. & Sachse D. (2013b) Leaf water deuterium enrichment shapes leaf
917 wax n-alkane δD values of angiosperm plants I: Experimental evidence and
918 mechanistic insights. *Geochimica Et Cosmochimica Acta* **111**, 39-49.

Kahmen A., Simonin K., Tu K.P., Merchant A., Callister A., Siegwolf R., Dawson T.E. & Arndt S.K. (2008) Effects of environmental parameters, leaf physiological properties and leaf water relations on leaf water $\delta^{18}O$ enrichment in different *Eucalyptus* species. *Plant Cell and Environment* **31**, 738-751.

Koeniger P., Marshall J.D., Link T. & Mulch A. (2011) An inexpensive, fast, and reliable method for vacuum extraction of soil and plant water for stable isotope analyses by mass spectrometry. *Rapid Communications in Mass Spectrometry* **25**, 3041-3048.

Lawrence J.R. & Gedzelman S.D. (1996) Low stable isotope ratios of tropical cyclone rains. *Geophysical Research Letters* **23**, 527-530.

Leaney F., Osmond C., Allison G. & Ziegler H. (1985) Hydrogen-isotope composition of leaf water in C_3 and C_4 plants: its relationship to the hydrogen-isotope composition of dry matter. *Planta* **164**, 215-220.

Lin G.H. & Sternberg L.S.L. (1993) Hydrogen isotopic fractionation by plant roots during water uptake in coastal wetland plants. In: *Stable isotopes and plant carbon-water relations* (eds J.R. Ehleringer, A.E. Hall, & G.D. Farquhar), pp. 497-510. Academic Press Inc., San Diego.

Loucos K.E., Simonin K.A., Song X. & Barbour M.M. (2015) Observed relationships between leaf $H_2{}^{18}O$ Péclet effective length and leaf hydraulic conductance reflect assumptions in Craig-Gordon model calculations. *Tree Physiology* **35**, 16-26.

Luz B. & Barkan E. (2011) The isotopic composition of atmospheric oxygen. *Global Biogeochemical Cycles* **25**.

Luz B., Barkan E., Yam R. & Shemesh A. (2009) Fractionation of oxygen and hydrogen isotopes in evaporating water. *Geochimica Et Cosmochimica Acta* **73**, 6697-6703.

Majoube M. (1971) Fractionnement en oxygen-18 et en deuterium entre l'eau et sa vapeur. *Journal de Chimie et Physique* **68**, 1423-1436.

Martín-Gómez P., Barbeta A., Voltas J., Peñuelas J., Dennis K., Palacio S., Dawson T.E. & Ferrio J.P. (2015) Isotope-ratio infrared spectroscopy: a reliable tool for the investigation of plant-water sources? *New Phytologist* **207**, 914-927.

McInerney F.A., Helliker B.R. & Freeman K.H. (2011) Hydrogen isotope ratios of leaf wax n-alkanes in grasses are insensitive to transpiration. *Geochimica Et Cosmochimica Acta* **75**, 541-554.

Merlivat L. (1978) Molecular diffusivities of $H_2{}^{16}O$, $HD^{16}O$, and $H_2{}^{18}O$ in gases. *Journal of Chemical Physics* **69**, 2864-2871.

952 Miller D.L., Mora C.I., Grissino-Mayer H.D., Mock C.J., Uhle M.E. & Sharp Z. (2006) Tree-
953 ring isotope records of tropical cyclone activity. *Proceedings of the National Academy*
954 *of Sciences of the United States of America* **103**, 14294-14297.
955 Munksgaard N.C., Cheesman A.W., Wurster C.M., Cernusak L.A. & Bird M.I. (2014)
956 Microwave extraction-isotope ratio infrared spectroscopy (ME-IRIS): a novel
957 technique for rapid extraction and in-line analysis of $\delta^{18}O$ and $\delta^{2}H$ values of water in
958 plants, soils and insects. *Rapid Communications in Mass Spectrometry* **28**, 2151-
959 2161.
960 Munksgaard N.C., Wurster C.M., Bass A. & Bird M.I. (2012) Extreme short-term stable
961 isotope variability revealed by continuous rainwater analysis. *Hydrological Processes*
962 **26**, 3630-3634.
963 Munksgaard N.C., Zwart C., Kurita N., Bass A., Nott J. & Bird M.I. (2015) Stable Isotope
964 Anatomy of Tropical Cyclone Ita, North-Eastern Australia, April 2014. *Plos One* **10**.
965 Ogée J., Barbour M.M., Wingate L., Bert D., Bosc A., Stievenard M., Lambrot C., Pierre M.,
966 Bariac T., Loustau D. & Dewar R.C. (2009) A single-substrate model to interpret
967 intra-annual stable isotope signals in tree-ring cellulose. *Plant Cell and Environment*
968 **32**, 1071-1090.
969 Ogée J., Cuntz M., Peylin P. & Bariac T. (2007) Non-steady-state, non-uniform transpiration
970 rate and leaf anatomy effects on the progressive stable isotope enrichment of leaf
971 water along monocot leaves. *Plant Cell and Environment* **30**, 367-387.
972 Orlowski N., Frede H.-G., Bruggemann N. & Breuer L. (2013) Validation and application of
973 a cryogenic vacuum extraction system for soil and plant water. *Journal of Sensors and*
974 *Sensor Systems* **2**, 179-193.
975 Pendall E., Williams D.G. & Leavitt S.W. (2005) Comparison of measured and modeled
976 variations in piñon pine leaf water isotopic enrichment across a summer moisture
977 gradient. *Oecologia* **145**, 605-618.
978 Ripullone F., Matsuo N., Stuart-Williams H., Wong S.-C., Borghetti M., Tani M. & Farquhar
979 G.D. (2008) Environmental effects on oxygen isotope enrichment of leaf water in
980 cotton leaves. *Plant Physiology* **146**, 729-736.
981 Rockwell F.E., Holbrook N.M. & Stroock A.D. (2014) The competition between liquid and
982 vapor transport in transpiring leaves. *Plant Physiology* **164**, 1741-1758.

983 Roden J., Kahmen A., Buchmann N. & Siegwolf R. (2015) The enigma of effective
984 pathlength for ^{18}O enrichment in leaf water of conifers. *Plant, Cell & Environment*,
985 n/a-n/a.
986 Roden J.S. & Ehleringer J.R. (1999) Observations of hydrogen and oxygen isotopes in leaf
987 water confirm the Craig-Gordon model under wide-ranging environmental conditions.
988 *Plant Physiology* **120**, 1165-1173.
989 Roden J.S., Lin G.G. & Ehleringer J.R. (2000) A mechanistic model for interpretation of
990 hydrogen and oxygen isotope ratios in tree-ring cellulose. *Geochimica et*
991 *Cosmochimica Acta* **64**, 21-35.
992 Rozanski K., Araguas-Araguas L. & Gonfiantini R. (1993) Isotopic patterns in modern global
993 precipitation. In: *Climate Change in Continental Isotopic Records* (eds P.K. Swart,
994 K.C. Lohmann, J. McKenzie, & S. Savin), pp. 1-36. American Geophysical Union,
995 Washington.
996 Sachse D., Billault I., Bowen G.J., Chikaraishi Y., Dawson T.E., Feakins S.J., Freeman K.H.,
997 Magill C.R., McInerney F.A., van der Meer M.T.J., Polissar P., Robins R.J., Sachs
998 J.P., Schmidt H.-L., Sessions A.L., White J.W.C., West J.B. & Kahmen A. (2012)
999 Molecular paleohydrology: interpreting the hydrogen- isotopic composition of lipid
1000 biomarkers from photosynthesizing organisms. *Annual Review of Earth and Planetary*
1001 *Sciences* **40**, 221-249.
1002 Sachse D., Gleixner G., Wilkes H. & Kahmen A. (2010) Leaf wax n-alkane δD values of
1003 field-grown barley reflect leaf water delta D values at the time of leaf formation.
1004 *Geochimica Et Cosmochimica Acta* **74**, 6741-6750.
1005 Sack L. & Holbrook N.M. (2006) Leaf hydraulics. In: *Annual Review of Plant Biology*, pp.
1006 361-381.
1007 Santos E., Wagner-Riddle C., Lee X., Warland J., Brown S., Staebler R., Bartlett P. & Kim
1008 K. (2014) Temporal dynamics of oxygen isotope compositions of soil and canopy
1009 CO_2 fluxes in a temperate deciduous forest. *Journal of Geophysical Research-*
1010 *Biogeosciences* **119**, 996-1013.
1011 Santrucek J., Kveton J., Setlik J. & Bulickova L. (2007) Spatial variation of deuterium
1012 enrichment in bulk water of snowgum leaves. *Plant Physiology* **143**, 88-97.
1013 Saurer M., Aellen K. & Siegwolf R. (1997) Correlating $\delta^{13}C$ and $\delta^{18}O$ in cellulose of trees.
1014 *Plant Cell and Environment* **20**, 1543-1550.

1015 Scoffoni C., Vuong C., Diep S., Cochard H. & Sack L. (2014) Leaf shrinkage with
1016 dehydration: coordination with hydraulic vulnerability and drought tolerance. *Plant*
1017 *Physiology* **164**, 1772-1788.
1018 Scrimgeour C.M. (1995) Measurement of plant and soil water isotope composition by direct
1019 equilibration methods. *Journal of Hydrology* **172**, 261-274.
1020 Seibt U., Wingate L., Berry J.A. & Lloyd J. (2006) Non-steady state effects in diurnal ^{18}O
1021 discrimination by *Picea sitchensis* branches in the field. *Plant Cell and Environment*
1022 **29**, 928-939.
1023 Simonin K.A., Roddy A.B., Link P., Apodaca R., Tu K.P., Hu J., Dawson T.E. & Barbour
1024 M.M. (2013) Isotopic composition of transpiration and rates of change in leaf water
1025 isotopologue storage in response to environmental variables. *Plant Cell and*
1026 *Environment* **36**, 2190-2206.
1027 Smith F.A. & Freeman K.H. (2006) Influence of physiology and climate on δD of leaf wax n-
1028 alkanes from C_3 and C_4 grasses. *Geochimica Et Cosmochimica Acta* **70**, 1172-1187.
1029 Snyder K.A., Monnar R., Poulson S.R., Hartsough P. & Biondi F. (2010) Diurnal variations
1030 of needle water isotopic ratios in two pine species. *Trees-Structure and Function* **24**,
1031 585-595.
1032 Song X., Barbour M.M., Farquhar G.D., Vann D.R. & Helliker B.R. (2013) Transpiration
1033 rate relates to within- and across- species variations in effective pathlength in a leaf
1034 water model of oxygen isotope enrichment. *Plant, Cell & Environment* **In press**.
1035 Song X., Clark K.S. & Helliker B.R. (2014) Interpreting species-specific variation in tree-
1036 ring oxygen isotope ratios among three temperate forest trees. *Plant Cell and*
1037 *Environment* **37**, 2169-2182.
1038 Song X., Loucos K.E., Simonin K.A., Farquhar G.D. & Barbour M.M. (2015a)
1039 Measurements of transpiration isotopologues and leaf water to assess enrichment
1040 models in cotton. *New Phytologist* **206**, 637-646.
1041 Song X., Simonin K.A., Loucos K.E. & Barbour M.M. (2015b) Modeling non-steady state
1042 isotope enrichment of leaf water in a gas-exchange cuvette environment. *Plant, Cell*
1043 *& Environment* **In press**.
1044 Sternberg L.S.L., Deniro M.J. & Johnson H.B. (1986) Oxygen and hydrogen isotope ratios of
1045 water from photosynthetic tissues of CAM and C_3 plants. *Plant Physiology* **82**, 428-
1046 431.

1047 Steudle E., Murrmann M. & Peterson C.A. (1993) Transport of water and solutes across
1048 maize roots modified by puncturing the endodermis- further evidence for the
1049 composite transport model of the root. *Plant Physiology* **103**, 335-349.
1050 Sturm P. & Knohl A. (2010) Water vapor δ^2H and $\delta^{18}O$ measurements using off-axis
1051 integrated cavity output spectroscopy. *Atmospheric Measurement Techniques* **3**, 67-
1052 77.
1053 Tang K.L. & Feng X.H. (2001) The effect of soil hydrology on the oxygen and hydrogen
1054 isotopic compositions of plants' source water. *Earth & Planetary Science Letters* **185**,
1055 355-367.
1056 Thomas E.M., Lin H., Duffy C.J., Sullivan P.L., Holmes G.H., Brantley S.L. & Jin L.X.
1057 (2013) Spatiotemporal patterns of water stable isotope compositions at the Shale Hills
1058 Critical Zone Observatory: linkages to subsurface hydrologic processes. *Vadose Zone*
1059 *Journal* **12**.
1060 Vendramini P.F. & Sternberg L. (2007) A faster plant stem-water extraction method. *Rapid*
1061 *Communications in Mass Spectrometry* **21**, 164-168.
1062 Walker C.D. & Lance R.C. (1991) The fractionation of ^2H and ^{18}O in leaf water of barley.
1063 *Australian Journal of Plant Physiology* **18**, 411-425.
1064 Walker C.D., Leaney F.W., Dighton J.C. & Allison G.B. (1989) The influence of
1065 transpiration on the equilibration of leaf water with atmospheric water vapor. *Plant,*
1066 *Cell and Environment* **12**, 221-234.
1067 Wang L.X., Good S.P., Caylor K.K. & Cernusak L.A. (2012) Direct quantification of leaf
1068 transpiration isotopic composition. *Agricultural and Forest Meteorology* **154**, 127-
1069 135.
1070 Wang X.F. & Yakir D. (1995) Temporal and spatial variation in the oxygen-18 content of
1071 leaf water in different plant species. *Plant, Cell and Environment* **18**, 1377-1385.
1072 Wang X.F., Yakir D. & Avishai M. (1998) Non-climatic variations in the oxygen isotopic
1073 composition of plants. *Global Change Biology* **4**, 835-849.
1074 Wassenaar L.I., Hendry M.J., Chostner V.L. & Lis G.P. (2008) High resolution pore water
1075 δ^2H and $\delta^{18}O$ measurements by $H_2O_{(liquid)}$-$H_2O_{(vapor)}$ equilibration laser spectroscopy.
1076 *Environmental Science & Technology* **42**, 9262-9267.
1077 Welker J.M. (2000) Isotopic ($\delta^{18}O$) characteristics of weekly precipitation collected across
1078 the USA: an initial analysis with application to water source studies. *Hydrological*
1079 *Processes* **14**, 1449-1464.

1080 Welp L.R., Keeling R.F., Meijer H.A.J., Bollenbacher A.F., Piper S.C., Yoshimura K.,
1081 Francey R.J., Allison C.E. & Wahlen M. (2011) Interannual variability in the oxygen
1082 isotopes of atmospheric CO_2 driven by El Nino. *Nature* **477**, 579-582.
1083 West A.G., Goldsmith G.R., Brooks P.D. & Dawson T.E. (2010) Discrepancies between
1084 isotope ratio infrared spectroscopy and isotope ratio mass spectrometry for the stable
1085 isotope analysis of plant and soil waters. *Rapid Communications in Mass*
1086 *Spectrometry* **24**, 1948-1954.
1087 West A.G., Goldsmith G.R., Matimati I. & Dawson T.E. (2011) Spectral analysis software
1088 improves confidence in plant and soil water stable isotope analyses performed by
1089 isotope ratio infrared spectroscopy (IRIS). *Rapid Communications in Mass*
1090 *Spectrometry* **25**, 2268-2274.
1091 West A.G., Patrickson S.J. & Ehleringer J.R. (2006a) Water extraction times for plant and
1092 soil materials used in stable isotope analysis. *Rapid Communications in Mass*
1093 *Spectrometry* **20**, 1317-1321.
1094 West J.B., Bowen G.J., Cerling T.E. & Ehleringer J.R. (2006b) Stable isotopes as one of
1095 nature's ecological recorders. *Trends in Ecology & Evolution* **21**, 408-414.
1096 White J.W.C. (1989) Stable hydrogen isotope ratios in plants: A review of current theory and
1097 some potential applications. In: *Applications of Stable Isotopes in Ecological*
1098 *Research* (eds P.W. Rundel, J.R. Ehleinger, & K.A. Nagy), pp. 142-160. Springer-
1099 Verlag, New York.
1100 Xiao W., Lee X.H., Wen X.F., Sun X.M. & Zhang S.C. (2012) Modeling biophysical controls
1101 on canopy foliage water ^{18}O enrichment in wheat and corn. *Global Change Biology*
1102 **18**, 1769-1780.
1103 Yakir D. (1992) Water compartmentation in plant tissue: Isotopic evidence. In: *Water and*
1104 *Life* (eds G.N. Somero, C.B. Osmond, & L. Bolis), pp. 205-221. Springer-Verlag,
1105 Berlin.
1106 Yakir D., Berry J.A., Giles L. & Osmond C.B. (1994) Isotopic heterogeneity of water in
1107 transpiring leaves: identification of the component that controls the $\delta^{18}O$ of
1108 atmospheric O_2 and CO_2. *Plant, Cell and Environment* **17**, 73-80.
1109 Yakir D., DeNiro M. & Gat J. (1990) Natural deuterium and oxygen-18 enrichment in leaf
1110 water of cotton plants grown under wet an dry conditions: Evidence for water
1111 compartmentation and its dynamics. *Plant, Cell and Environment* **13**, 49-56.

1112 Yakir D., Deniro M.J. & Rundel P.W. (1989) Isotopic inhomogeneity of leaf water: evidence
1113 and implications for the use of isotopic signals transduced by plants. *Geochimica et*
1114 *Cosmochimica Acta* **53**, 2769-2773.
1115 Zwieniecki M.A., Brodribb T.J. & Holbrook N.M. (2007) Hydraulic design of leaves:
1116 insights from rehydration kinetics. *Plant Cell and Environment* **30**, 910-921.
1117
1118

Table 1. Symbols and abbreviations used in the text.

Δ_e	Isotopic enrichment of evaporative site water compared to source water
Δ_L	Isotopic enrichment of bulk leaf water compared to source water
Δ_{Ln}	Predicted non-steady state isotopic enrichment of bulk leaf water
Δ_v	Isotopic enrichment of vapour compared to source water (typically negative)
δ_E	$\delta^{18}O$ or $\delta^{2}H$ of transpired water vapour
δ_L	$\delta^{18}O$ or $\delta^{2}H$ of bulk leaf water
δ_e	$\delta^{18}O$ or $\delta^{2}H$ of water at the evaporative sites within leaves
δ_s	$\delta^{18}O$ or $\delta^{2}H$ of source water
δ_v	$\delta^{18}O$ or $\delta^{2}H$ of atmospheric vapour
$\delta^{18}O$	$^{18}O/^{16}O$ relative to the value of a standard (VSMOW for plant waters)
$\delta^{2}H$	$^{2}H/^{1}H$ relative to the value of a standard (VSMOW for plant waters)
ε^{+}	Equilibrium isotope fractionation between liquid water and vapour
ε_k	Kinetic isotope fractionation caused by diffusion of water vapour in air
$\wp$	The Péclet number (representing the ratio between advection and diffusion)
E	Transpiration rate
L	Effective path length for water movement through the mesophyll
W	Leaf water concentration
g	Stomatal conductance to water vapour
w_a	Water vapour mole fraction in the atmosphere
w_i	Water vapour mole fraction in the intercellular air spaces inside leaves

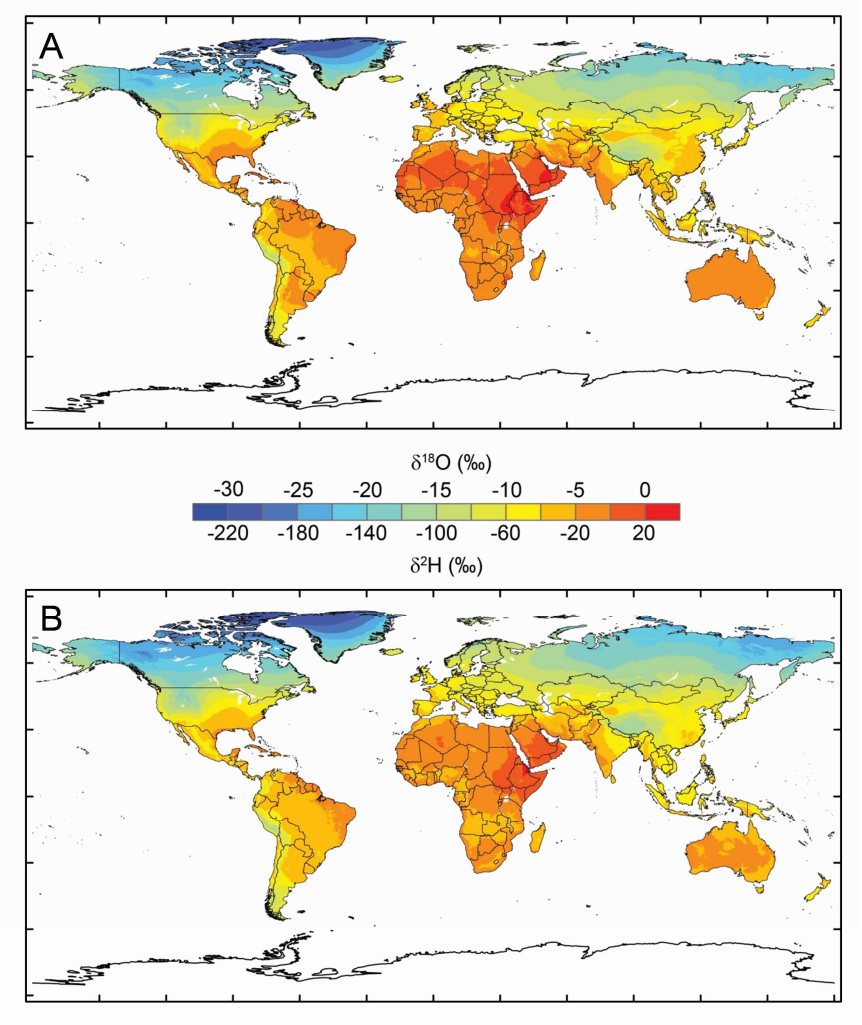

Figure 1. Spatial distribution of hydrogen and oxygen isotope ratios of precipitation over land. These precipitation isoscapes were derived from a long-term, global network of observations (Welker 2000; IAEA/WMO 2011) and a geostatistical and regression-based model developed with the online workspace IsoMAP (Isoscapes Modeling, Analysis and Prediction v 1.0; http://isomap.org). Model structure, statistical results, and isoscapes may be accessed or downloaded from IsoMAP by referencing job keys: 48170, 48171, 48236, and 48560 (West, 2015).

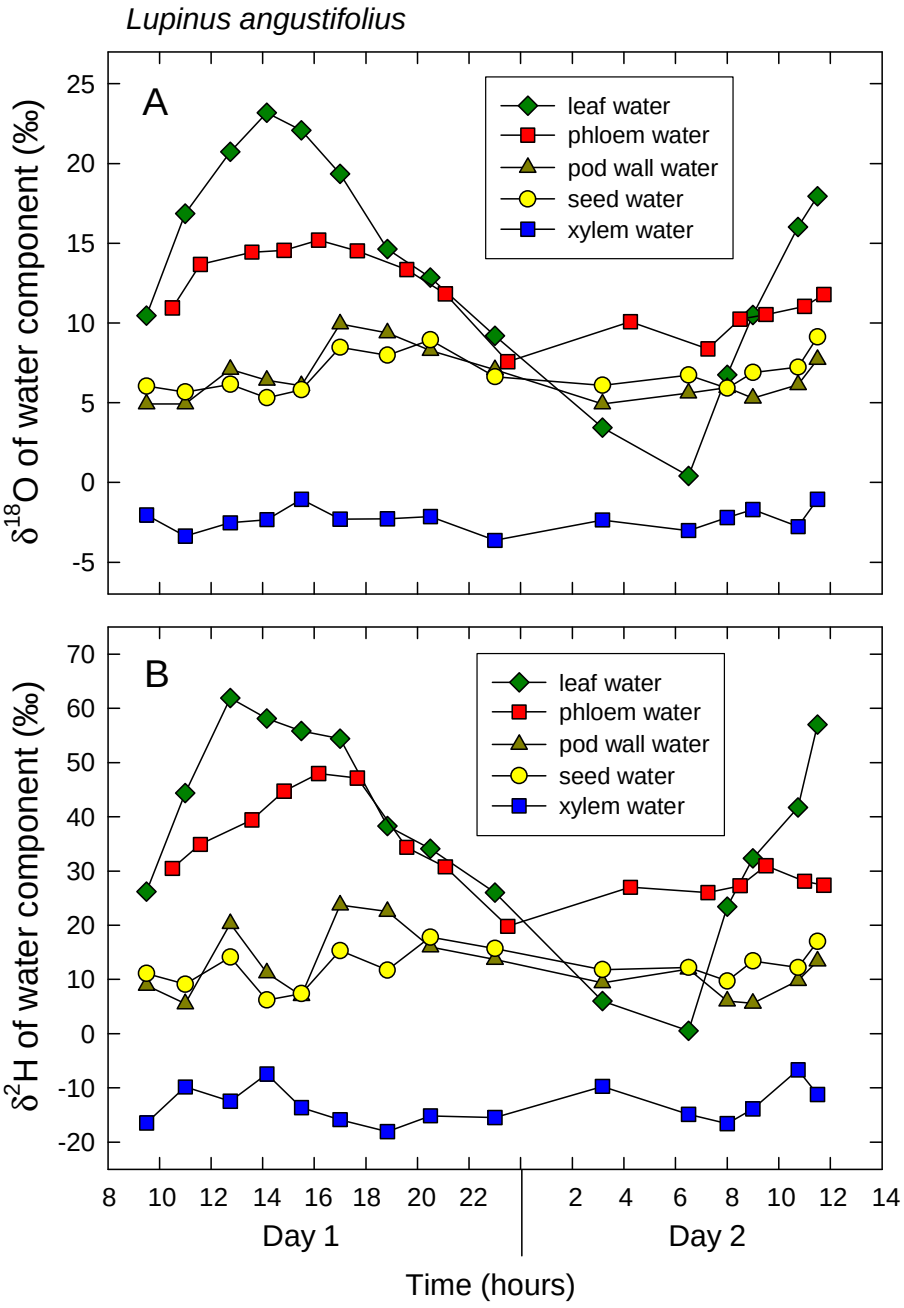

Figure 2. Diel variation in leaf, phloem, pod wall, seed, and xylem water $\delta^{18}O$ (A) and $\delta^{2}H$ (B). Samples were collected in Western Australia from *Lupinus angustifolius* grown as part of an agricultural trial. Phloem sap was sampled from pod tips, using a phloem bleeding technique. Redrawn from Cernusak et al. (2002).

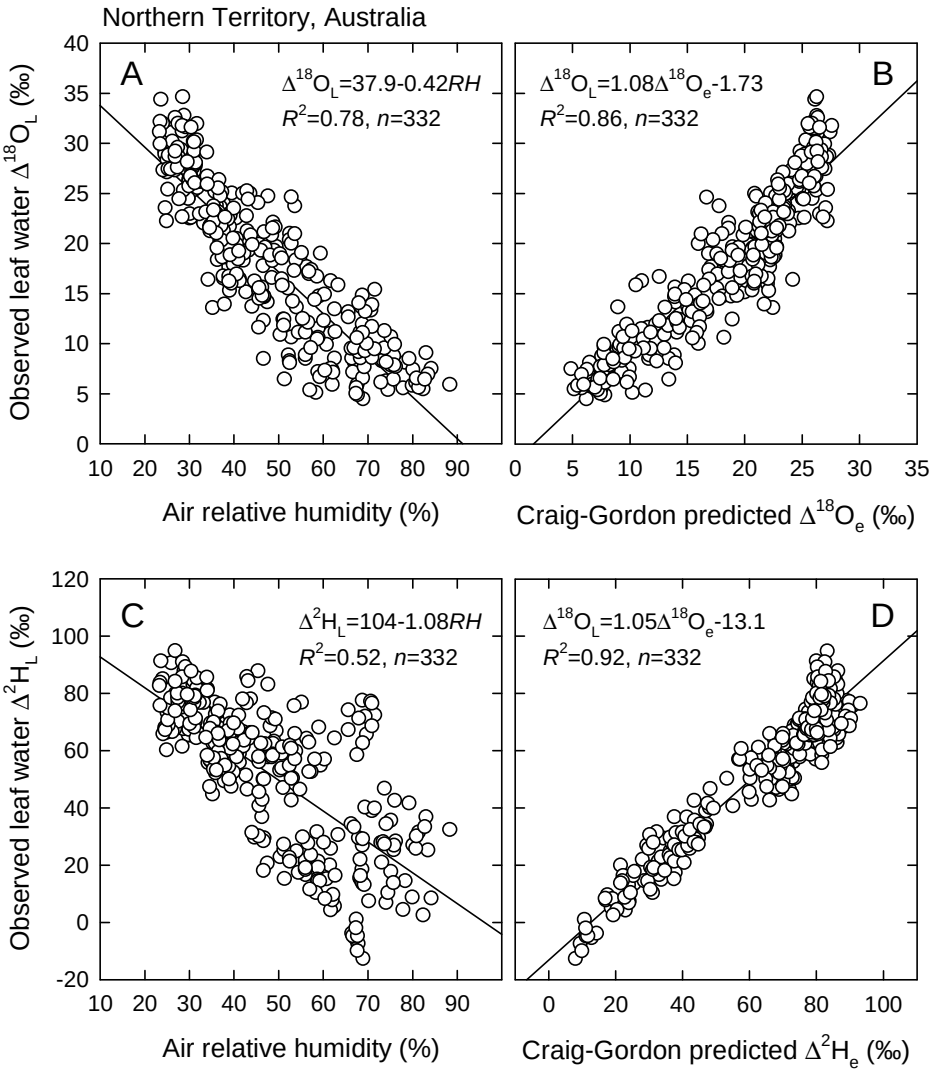

Figure 3. Relationships between observed leaf water stable isotope enrichment for oxygen ($\Delta^{18}O_L$) and hydrogen (Δ^2H_L) and the relative humidity of the air recorded at the time of sampling (A and C) and the Craig-Gordon predicted enrichments (B and D). Craig-Gordon predicted enrichments were calculated with Eqn 4 of the main text. Samples were collected during daytime from various *Eucalyptus* and *Acacia* species distributed over a sub-continental rainfall gradient in northern Australia (Kahmen *et al.* 2013a). The full dataset is provided in the Supplementary Material. Panel D is redrawn from Kahmen et al. (2013a).

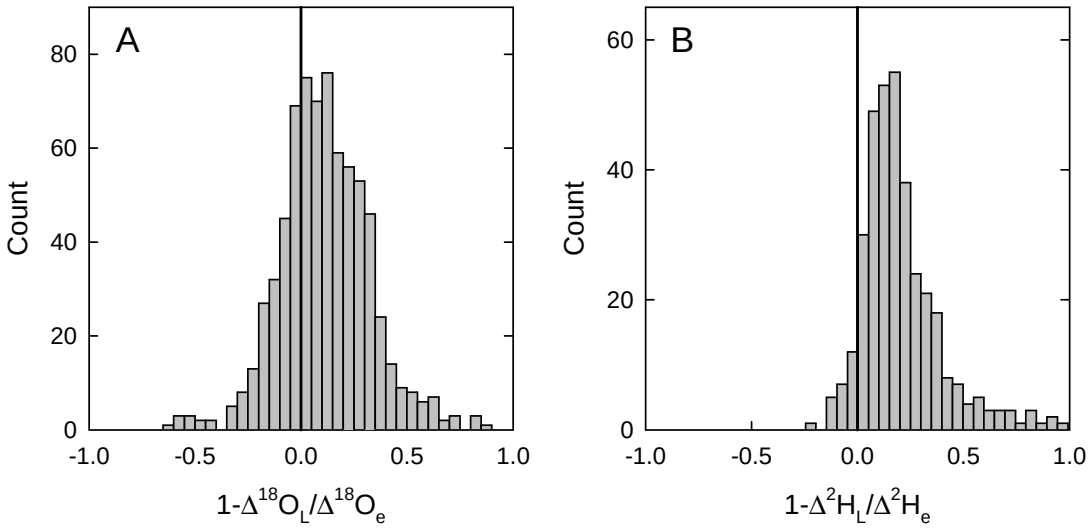

Figure 4. Histograms showing the proportional difference between Craig-Gordon predicted leaf water stable isotope enrichment ($\Delta^{18}O_e$ and $\Delta^{2}H_e$) and observed bulk leaf water enrichment ($\Delta^{18}O_L$ and $\Delta^{2}H_L$) for $\Delta^{18}O$ (A) and $\Delta^{2}H$ (B). Craig-Gordon predicted enrichments were calculated with Eqn 4 of the main text. The dataset combines observations from several publications (Wang, Yakir & Avishai 1998; Cernusak *et al.* 2002; Cernusak *et al.* 2005; Kahmen *et al.* 2008; Kahmen *et al.* 2011; Kahmen *et al.* 2013a; Song *et al.* 2013; Song *et al.* 2014). The full dataset is provided in the Supplementary Material.

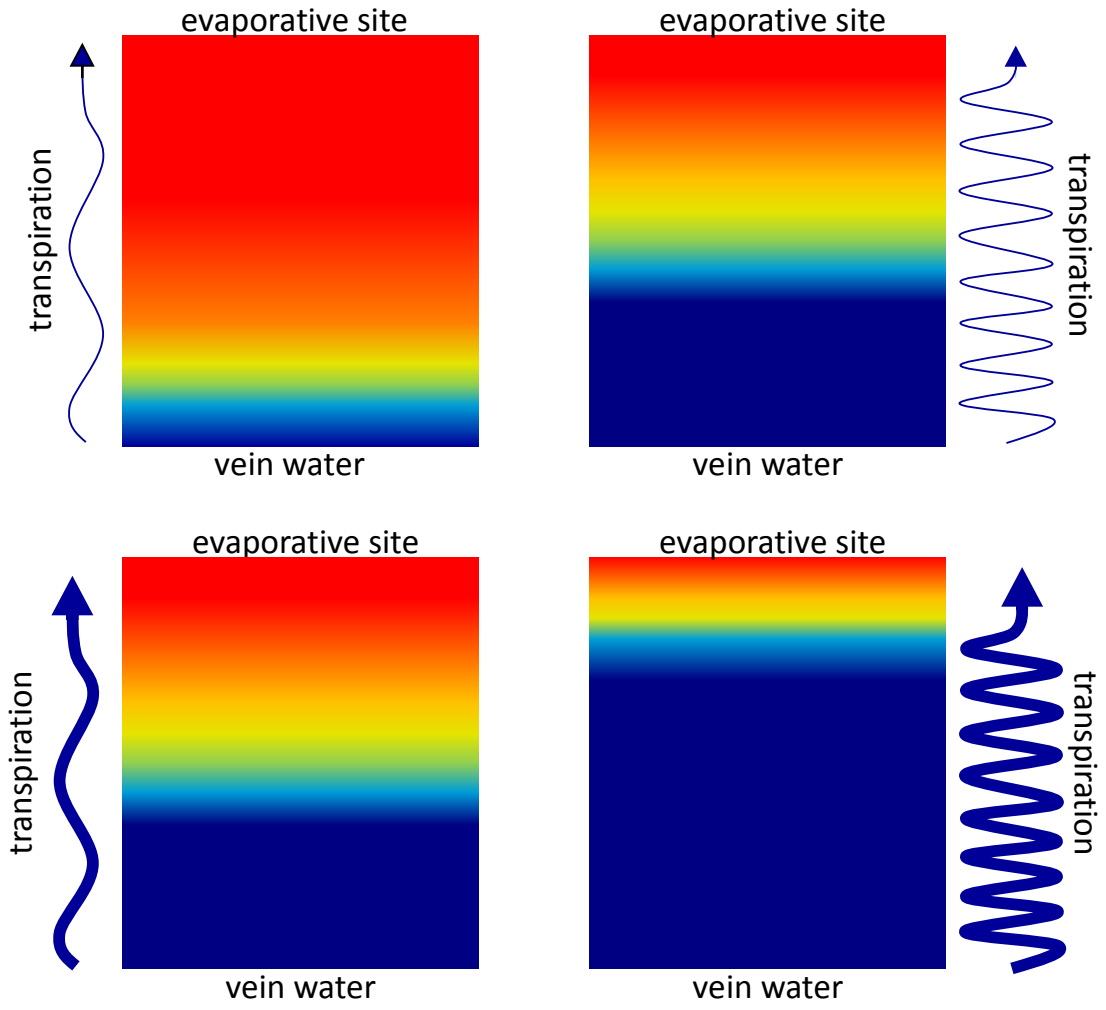

Figure 5. A schematic representation of the Péclet model of leaf water stable isotopic enrichment (Farquhar & Lloyd 1993). The model describes the average lamina leaf water ^{18}O and ^{2}H enrichment relative to that at the evaporative sites as a function of the interplay between diffusion of isotopically enriched water away from the evaporative sites and advection of unenriched vein water toward the evaporative sites. The vein water is transported along a path, the length of which varies as a function of its tortuosity. The average lamina leaf water ^{18}O and ^{2}H enrichment decreases if the transpiration rate is high, or when the scaled effective path length is long. Either of these conditions will impede the diffusion of isotopically enriched water away from the evaporative sites. In the figure, red represents the highest ^{18}O and ^{2}H enrichment, yellow intermediate, and blue the lowest. The thickness of arrows indicates transpiration rates and the sinuosity of arrows indicates scaled effective path lengths. Redrawn from Cernusak and Kahmen (2013).

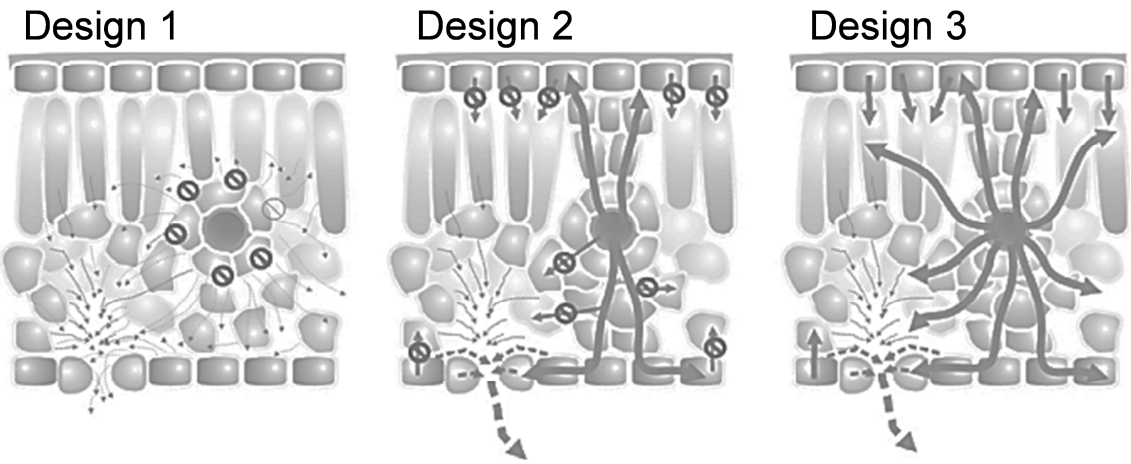

Figure 6. Schematic of three scenarios for leaf hydraulic design describing the hydraulic linkages between different tissues. The dark grey circle in the middle is a water-filled vein, solid lines depict water flow, with the thicker lines corresponding to higher flow, dashed lines describe diffusion of water vapour, and Ø denotes high resistance between tissue types. In Design 1, the vein is relatively isolated hydraulically from the rest of the leaf; in Design 2, the epidermal tissues are hydraulically linked to the vein by the bundle sheath extensions, but the mesophyll remains relatively isolated; and in Design 3, all tissues are equally well linked hydraulically. Reprinted from Zwieniecki et al. (2007).

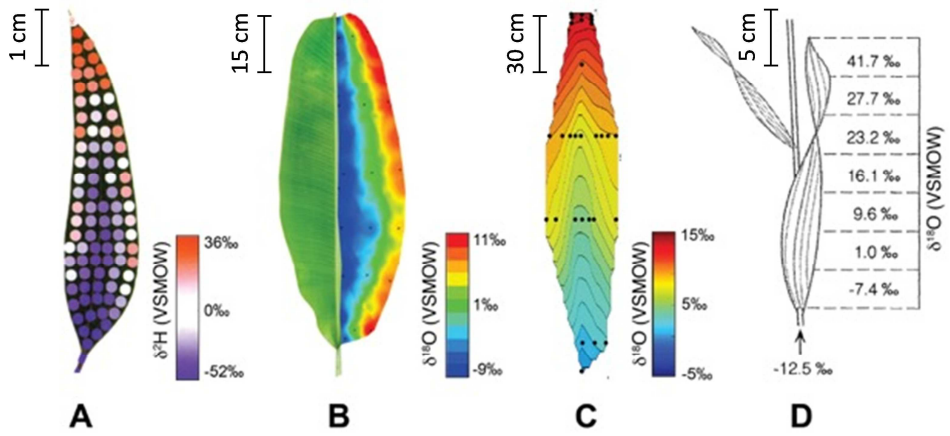

Figure 7. Spatial variation in leaf water isotopic composition in a tree leaf, *Eucalyptus pauciflora* (A), a banana leaf, *Musa* sp. (B), a cactus stem, *Carnegiea gigantea* (C), and a grass blade, *Miscanthus sinensis* (D). Progressive isotopic enrichment from the base to the apex of the leaf/stem and from the middle toward the edges of the leaf/stem is a common feature. Note that in the banana leaf, the progressive enrichment shows in the perpendicular direction to the midrib, rather than along its length. The left side of the banana leaf shows the vein patterning. Scale bars are approximate. Figures are modified from Santrucek *et al*. (2007), Stuart-Williams (unpublished), English *et al*. (2007), and Helliker and Ehleringer (2000), respectively.

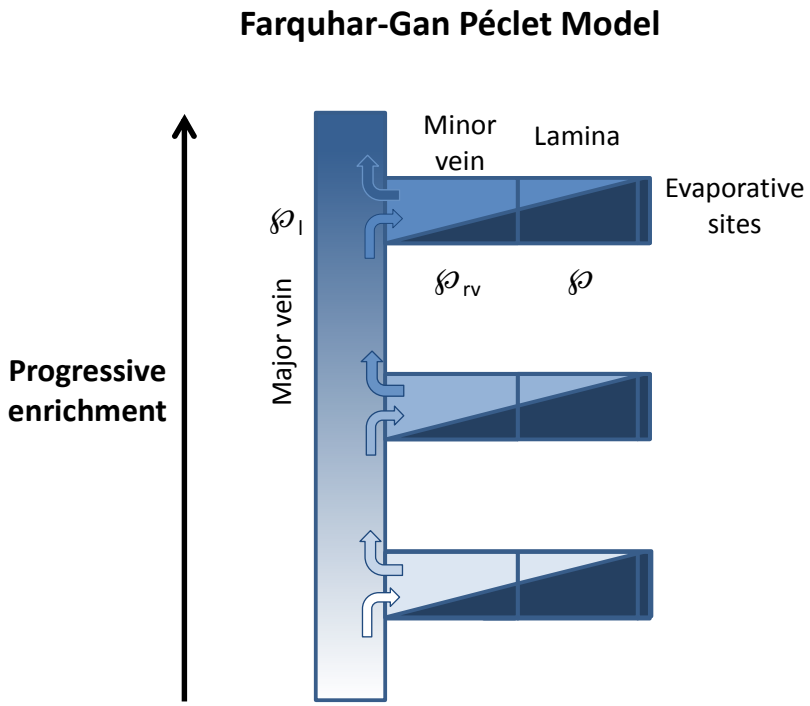

Figure 8. A schematic representation of the Farquhar and Gan (2003) Péclet model that predicts progressive enrichment of leaf water stable isotopes along a leaf. Darker blue indicates a higher level of stable isotope enrichment. In the model, isotopically lighter water is preferentially transpired leaving heavier water to diffuse back into the xylem and be carried further along the leaf. For this pattern to be pronounced, the ratio of advection to diffusion (Péclet number) has to be large in the longitudinal direction, and small in the radial direction. In the figure, $\wp_l$ is the longitudinal Péclet number, $\wp_{rv}$ is the radial Péclet number associated with veinlets, and $\wp$ is the radial Péclet number associated with the mesophyll in the leaf lamina.